Consistency of Aerial LiDAR-Derived Forest Metrics Across Multiple Acquisitions

Luke Dow

A thesis

Submitted in partial fulfillment of the

Requirements for the degree of:

Master of Science

University of Washington

2015

Committee:

Jerry F. Franklin

Van Kane

Robert McGaughey

Ernesto Alvarado

Program Authorized to Offer Degree:

School of Environmental and Forest Sciences

University of Washington

Abstract

Consistency of Aerial LiDAR-Derived Forest Metrics Across Multiple Acquisitions

Luke Dow

Chair of supervisory committee:
Dr. Jerry Franklin
School of Environmental and Forest Sciences

As remote sensing technology advances, there is growing interest in using LiDAR to compare structural attributes between forest ecosystems and to monitor forests following active management. However, these emerging applications cannot be confidently employed without quantification of the consistency of repeat LiDAR acquisitions. To address this problem, I explore the impact of different sensors, flight directions, and flight altitudes on LiDAR-derived metric and canopy surface model consistency in the Dinkey Creek Watershed. In addition, I analyze whether structural changes in the forest are detected by LiDAR metrics. I conduct metric comparisons at 15-, 30-, and 46-meter resolutions and canopy surface model comparisons at 1-, 2-, and 3-meter resolutions to determine if processing pixel size affects metric consistency. The results show that collecting LiDAR using different sensors, flight directions, and flight altitudes does not reduce the stability of the metrics. Elevation percentile metrics, canopy proportion metrics, structure classes, and canopy rumple metrics maintain > 0.90 coefficient of determination (R^2) values; and elevation mean, elevation standard deviation, and total cover > 2 meters maintain R^2 values above 0.95 between acquisitions collected two years apart. Additionally, the R^2 values of the canopy proportion metrics are lower in areas harvested between acquisitions, indicating these metrics reflect structural changes in the forest. Metric consistencies increase with pixel size, from 15-46 meters. Canopy surface model consistency varies, but maintains R^2 values above 0.90 for pixel sizes ranging 1-3 meters.

Introduction

The size, spatial arrangement, and stratification of live trees, standing dead trees, and downed woody debris in forests is commonly referred to as forest structure. Understanding the structure of an ecosystem is a crucial piece of understanding forest dynamics because it reflects stand history, vegetative species diversity, and ecosystem function (Spies 1998, Franklin and Spies 1991, Lindenmayer and Franklin 2002, McElhinny et al 2005, Kane et al. 2010a).

Light detection and ranging (LiDAR) collects elevation data for surfaces and objects illuminated by laser pulses, which can be used to extrapolate tree height, canopy width and stratification, and tree density (Lefsky et al. 2001, Reutebuch et al. 2005). These are fundamental attributes of forest structure, LiDAR is gaining momentum among forest managers and researchers as a method to map and quantify structural attributes in forest ecosystems. As the technology advances and interest grows, research for new LiDAR and remote sensing applications is in demand. In particular, forest managers conducting restorative projects have expressed interest in using multiple LiDAR acquisitions to compare structural attributes of ecosystems and to monitor forest dynamics (Reutebuch et al. 2003, Naesset 2004, St-Onge et al. 2004).

An underlying assumption when comparing multiple LiDAR acquisitions is that measurements are accurate, precise, and repeatable. Studies have shown LiDAR is accurate and precise within a single acquisition (Aldred and Bonner 1985, Nilsson 1996, Magnussen and Boudewyn 1998); however the repeatability assertion is, for the most part, untested. Each LiDAR acquisition is unique, yielding intrinsic differences among datasets. Furthermore, acquisition specifications are not standardized, which increases potential for inconsistency. Flight specifications such as sensor type, scan angle, beam divergence, flight altitude, pulse density, and time of year can alter how stand properties are sensed (Naesset et al. 2004, Naesset et al. 2005, Goodwin et al. 2006, Chasmer et al. 2006, Hopkinson 2007,

Magnussen et al. 2007, Gobakken et al. 2008, Nelson et al. 2011). These differences may render direct comparisons unreliable, which presents difficulties for structural comparisons and temporal monitoring.

Having confidence in using LiDAR-derived metrics from multiple acquisitions for ecosystem comparison and monitoring is contingent on empirical evidence that LiDAR acquisitions are consistent. Toward this end, my project investigates the consistency of LiDAR acquisitions on multiple levels. I compare the overlapping area between flight lines within a single acquisition in the initial step of my study (Figure 1). This method omits temporal influences, allowing for direct exploration of consistency by acquisition specification. I conduct comparisons between overlapping areas of the Dinkey Creek Watershed 2010 and 2012 acquisitions in the second step of my study. This method introduces temporal influences, allowing for a more complex evaluation of LiDAR consistency. These comparisons are used to explore the following questions:

1.) Which acquisition specifications contribute to metric inconsistency?
2.) Which metrics maintain consistency, and which are less stable across time?
3.) Is there correlation between return height in canopy and metric consistency?
4.) Which metrics are sensitive to timber harvest /structural changes?
5.) Does metric resolution alter consistency?

An analysis of these results will expose the primary sources of error, and will provide a baseline set of metrics that maintain the highest consistency between acquisitions.

Methods

Study site

Watershed Sciences, Inc. collected LiDAR in 2010 and 2012 of the Dinkey Creek/Tea Kettle study area in the Sierra National Forest for the USDA Forest Service (Figure 2). The Dinkey Creek watershed is a south-trending 35,410-hectare tributary channel of the King River located in the Sierra National Forest in the southern Sierra Nevada Mountains. The climate is Mediterranean, characterized by warm dry summers and cold wet winters.

The Dinkey landscape encompasses the full range of vegetation types found in the Sierra Nevada: coniferous forest, foothill hardwood and chaparral vegetation, and montane meadows and riparian forests. Approximately 64% of the landscape is mixed-conifer and ponderosa pine forests, composed largely of white fir (*Abies concolor*) with ponderosa pine (*Pinus ponderosa*), Jeffrey pine (*Pinus Jeffreyi*), sugar pine (*Pinus lambertiana*), incense cedar (*Calocedrus decurrens*), and red fir (*Abies magnifica*). 23% is chaparral or hardwood, approximately 1% are meadow, and 10% are rock/thin soil. The elevation ranges approximately from 250 to 3000 meters (Dinkey Landscape Restoration Project).

LiDAR Data

The Dinkey 2010 acquisition covers 20,911 hectares (80.7 $mi.^2$), and was buffered to ensure full coverage, resulting in a total area flown of 23,867 hectares (92.2 $mi.^2$) (Figure 2). Acquisition dates were October 12-19, 2010. The LiDAR survey utilized dual-mounted LEICA ALS50 Phase II sensors. Discrete portions of the area were flown at 1100 and 1500 meters above ground level, capturing a maximum scan angle of ~14^o from nadir. The Leica systems were set to acquire >83,000 pulses/second. The total average and ground pulse density statistics for the study are 8.8 total pulses per square meter, and 0.89

ground pulses per square meter. The area was surveyed with opposing flight line side-lap of 50% to reduce laser shadowing and increase surface laser painting.

The Dinkey 2012 acquisition covers 24,086 hectares (92.9 mi.^{2}), but was also buffered, resulting in a total area flown of 24,937 hectares (96.3 mi.^{2}) (Figure 2. Acquisition dates were November 21-27, 2012. The LiDAR survey utilized a Leica ALS 60 sensor system. The flying altitude was 900 m, and captured a maximum scan angle of 14^o from nadir. The resulting laser pulse diameter was 21 cm at ground level. The target pulse rate was 96.0-105.9 kHz, yielding 8 pulses/m^2. The area was surveyed with opposing flight line side-lap of 50% to reduce laser shadowing and increase surface laser painting. There was a dusting of snow cover < 1 inch deep at higher elevations during this acquisition.

Watershed Sciences created multiple products from the raw Dinkey 2010 and 2012 LiDAR data for the USDA Forest Service (see Appendix 1 for full list of products).

Deriving metrics and structure classes

To test the impact of map resolution on the consistency of derived information, the raw data for each LiDAR acquisition were processed to derive 202 height, strata, and intensity metrics at three resolutions: 15-meter, 30-meter, and 46-meter. A 2-meter height cutoff was used when calculating the LiDAR metrics. That is, only points higher than two meters above the ground surface were used to compute the majority of the metrics. The number of returns for each strata layer (1-2m, 2-4m, 4-8m, 8-16m, 16-32m, 32-64m, >64m) were used to calculate the proportion of canopy cover in each height bracket, using the equation:

$$\text{cover\_n} = \frac{\text{strata\_n}}{\text{strata\_n}+\text{strata\_n}-1+\ldots+\text{strata\_1}}$$

Equation 1: Canopy proportion metric derivation.

Where cover_n is the percent cover in strata layer “n”, and strata_n is the total number of returns in strata layer “n”. These metrics will be referred to as the cover metrics. All raw data processing was conducted with FUSION (McGaughey 2014).

Structure classes are derived metrics that represent the spatial arrangement of structures in a forest. There is interest in using structure classes to analyze forest characteristics, so the structure classes, and the metrics used to derive them, are a focus of this paper. The structure classes were derived from 13 metrics that had been identified in other studies as key for distinguishing forest structural conditions to derive structural classes (Kane et al. 2010a, Kane et al. 2013) (Figure 3). The metrics were selected from three categories of metrics found by Lefsky et al. (2005) to be highly correlated with field measurements of stand structure: height, variation of height, and canopy density (Kane et al 2010a).

The structural classes were derived from a random sample of 25,000 grid cells, and from combined metrics that included data from both the 2010 and 2012 acquisition. A distance matrix was created using Euclidean distances within the vegdist function in the vegan R statistical package (Oksanen et all. 2015). Hierarchical clustering, which defines classes by grouping the most similar observations (Legendre and Legendre 1998), was conducted on the distance matrix. The clustering algorithm used the Ward agglomerative minimum variance approach within the hclust function of the R statistical package (release 2.6.1) (R Development Core Team 2007). A random forest model was created using the combined 2010 and 2012 metrics. However, the results were imputed (using the yaImpute R statistical package) using the separated 2010 and 2012 metrics, creating structure maps for each acquisition. This imputation related the classes to predictors and created a spatial distribution map of the classes across each independent acquisition.

A principal component analyses (PCA) was conducted to explore the multivariate relationships among the classes. A qualitative inspection of the structure class part plots was used to determine the number

of structure classes necessary to most effectively describe the variation over the landscape while minimizing redundancy.

Deriving Canopy Surface Model

Canopy surface models (CSMs) were created for each study site from first returns using three resolutions: 1.0, 2.0, and 3.0 m; a 3 x 3 smoothing algorithm was applied to each resolution (Kane et al. 2010a). These parameters provided realistic canopies over the range of canopy types and pulse densities in the study. The cell sizes were chosen to ensure that consistency is stable across a range of resolutions. Smoothing eliminated the jagged, unnatural canopy surface that is common when moderate- density LiDAR data are used without smoothing, such as ‘‘pits’’ within tree crowns due to small gaps that permit a first return from the ground surface (Kane et al. 2010a).

Ground Model Stability

Before comparisons were conducted, the ground models were tested for consistency between acquisitions. This underlying layer provides a basis for the elevation measurements, so is an imperative component of the comparisons. Statistical analyses to test the stability included differences and least squares linear regressions between associated pixels. A 99.9% confidence interval was conducted to test whether the slope differs from 1.0 and whether the y-intercept differs from 0.0. The 99.9% level was chosen because maximum model accuracy is necessary in this fundamental comparison.

2010 Flight line comparisons

The Dinkey 2010 metrics were processed at 15-meter resolution, 30-meter resolution, and 46-meter resolution to understand trends of consistency with resolution. The intent of the flight line comparisons however is to provide baseline consistency, rather than trends. Reporting the full analyses of multiple resolutions would be redundant, so I compared flight lines at the 30-meter resolution. The FUSION tool

clipdata was used to extract 30-meter square samples along the flight line interface and along the elevation interface to conduct comparisons (FUSION version 3.42, Bob McGaughey 2014) (Figure 4).

Multiple levels of comparison were conducted to more effectively isolate inconsistencies by source. The 2010 acquisition specifications allow three levels of similarity to be investigated between the flight lines: 1.) flight lines 106 and 107 were collected with the same sensor, but points were collected from different angles; 2.) flight lines 106 and 1109 were collected from the same direction, but using different sensors; and 3.) flight lines 39 and 75 were collected at 1100- and 1500-meter altitudes respectively, using the same sensor. Comparisons using flight lines 106, 107, and 1109 use 232 samples extracted from the flight line overlap. Comparisons using flight lines 39 and 75 use 239 samples extracted from the flight line overlap.

Differences, subtracting the values in corresponding samples between two flight lines, and ordinary least square regressions were conducted between corresponding samples to determine consistency of the direct metrics (height and intensity metrics extracted directly from the LiDAR point cloud) and the derived metrics (cover metrics, which are derived from the direct metrics). I used the linear model: yi = xi+0, the line representing equality between the flight line metrics. This allowed exploration of whether the points from each flight line had a 1:1 relationship.

The analyses were also used to determine if consistency varies with absolute height (strata layer) and relative height (height percentile returns) in canopy. Eight metrics (elevation 25^{th}, 50^{th}, and 95^{th} percentile return heights; elevation mean and standard deviation; cover metrics 2-4m, 8-16m, and 32-64m) were chosen to represent the trends of each acquisition comparison.

Dinkey 2010 vs. 2012 Comparisons

The comparisons between the Dinkey Creek Watershed 2010 and 2012 LiDAR datasets were conducted on overlapping portions of the 2010 and 2012 acquisitions (Figure 5). The overlaps were identified and isolated using the Extract by Mask tool in ArcMap. Areas of overlap were reduced (buffered) by 100 meters to reduce edge effects. After buffering, the overall area for comparison was 5133 hectares. Regions that underwent major ecosystem changes (such as harvest or disturbance) were masked and compared separately from the unaltered portions of the acquisitions. This allowed an analysis of how changes in ecosystem are reflected by the metrics and structure classes. The harvest area compared was 650 hectares, and the unharvested area compared was 4483 hectares. Corresponding pixels from each acquisition were compared to determine consistency. The resolution of the metrics and structure classes is 30 m^2 and the resolution of the canopy height models is 1 m^2.

Ordinary least square regressions were conducted to determine the overall consistency of direct metrics, derived metrics, and structure classes. In conducting the linear regression, I fit the points to the linear model: yi = xi+0. This allowed exploration of whether the points from each acquisition had a 1:1 relationship. Differences, calculated by subtracting corresponding pixels in the 2012 acquisition from the 2010 acquisition (displayed in difference maps) were used to calculate the absolute changes and to visualize the distribution of the differences across the landscape.

The analyses were also used to determine if consistency varies with absolute height (strata layer) and relative height (height percentile returns) in canopy. 11 representative metrics (the elevation mean, standard deviation, and 25^{th}, 50^{th}, and 95^{th} percentile return heights; the cover metrics 2-4m, 8-16m, and 32-64m; and the rumple and structure classes) were chosen to display the trends of each acquisition comparison. Comprehensive results will be discussed for the 30-meter resolution comparisons, but only

trends in relation to this resolution will be discussed regarding the 15-meter and 46-meter resolution comparisons.

The higher resolution of the canopy surface model necessitated segmentation of the area into 9 blocks for processing, however only 4 segments contained overlapping points: blocks 1, 2, 4, and 5. The blocks are 3.7 hectares, 387.6 hectares, 610.3 hectares, and 2552.2 hectares in area respectively (Figure 6). Differences and ordinary least squared regressions were conducted to compare each pixel in the 2010 acquisition with corresponding pixels in the 2012 acquisition.

Different resolutions

The raw LiDAR data was processed using a 15-, 30-, and 46-meter resolutions and the canopy surface model was processed at 1-, 2-, and 3-meter resolutions. Ordinary least squares regressions were conducted to for each resolution determine overall consistency. Differences, calculated by subtracting corresponding pixels in the 2010 acquisition from the 2012 acquisition (displayed in difference maps) were used to calculate the absolute changes and to visualize the distribution of the differences across the landscape. The canopy surface model 2-meter and 3-meter r^2 values were derived in a 1,000 m^2 portion of block 2 to avoid bias due to landscape changes. The consistencies reported in the resolution trends are in only unharvested regions.

Results

Structure classes

The bar plots derived from the hierarchical clustering algorithm indicated 9 structure classes most effectively describe the acquisitions. A suite of tables and figures produced using RStudio and ArcMap provides an accessible format to understand the LiDAR metrics, structural classes, and forest conditions. Appendix 2 contains the structure class characteristics.

Ground Model Stability

The ground model comparison shows there is high correlation between the acquisitions. The r^2 value rounds to 1.0, the t-value is 36,306, and the p-value is 2.2e-16 (Table 1). Additionally, The 99.9% confidence interval indicates the y-intercept is between -0.198 and 0.140 and the slope is between 0.999 and 1.000.

Dinkey 2010 flight line comparisons

The first comparison involved using the same sensor, but acquiring points from opposing directions (flight lines 106 and 107). Eight metrics representing the elevation percentiles and and cover proportions show a trend of increasing r^2 values with height in the canopy (Figure 7). All metrics maintain R^2 values above 0.90 except cover in the 2-4m strata layer.

The second comparison involved using different sensors, but collecting points nearly simultaneously and from the same direction (flight lines 106 and 1109). Again, the 8 representative metrics show a trend of increasing r^2 values with elevation in the canopy for the elevation and cover proportion metrics (Figure 7). Cover in the 2-4m strata layer has an R^2 value above 0.90, indicating consistency when collecting LiDAR from the same direction.

The third comparison involved using the same sensor, but collecting points at different flying altitudes and from different directions (flight lines 39 and 75). The elevation percentile returns all have R^2 values of 0.99, so there is no definite trend regarding height in canopy (Figure 7). The cover metrics however, do show a trend of increasing consistency with canopy height. Cover in the 2-4m strata layer has a lower R^2 value, indicating less consistency.

Dinkey 2010 vs. Dinkey 2012 metric comparisons

Overall Area

The first inter-acquisition comparisons, which include two years of temporal influence, were conducted over the entire overlapping portion of the Dinkey 2010: Dinkey 2012 overlap to more thoroughly explore LiDAR acquisition consistency. Average metric consistency is lower than between the flight lines (Table 3), however similar trends emerge regarding canopy height. The elevation percentile return heights and cover metrics suggest consistency increases with canopy height. The return count metric r^2 values range from 0.32 to 0.50 and do not trend regarding return number. The intensity metrics range from 1.2e-4 to 5.5e-3 and do not show trend based on percentile return value. The structure classes and rumple have r^2 values of 0.92 and 0.89 respectively (Figure 8).

Scatter plots comparing the 2010 and 2012 data provide point distribution visualizations. The overall plots show the trend of increasing consistency with height in canopy. The 32-64m cover proportion plot is evenly distributed across the 1:1 line. The 8-16m proportion plot is weighted toward the 2010 acquisition, particularly between 2010 values 0.1 and 0.4. The 2-4 m proportion plot also shows skew toward the 2010 acquisition. The elevation percentile returns are points evenly distributed across the 1:1 line. The intensity p95 plot indicates there is little discernible correlation between the acquisitions and the total return proportion plot shows decreasing correlation with number of returns. The rumple and structure class points are evenly distributed across the 1:1 line (Figure 9).

Unharvested Area

The second analysis was conducted over the unharvested area to show the consistency of metrics without influence from structural changes. The average metric consistency is higher than both the overall comparison and the harvested area comparison (Table 3). The elevation return percentiles maintain r^2 values above 0.90 from the 25^{th} percentile to the 95^{th} percentile and the canopy proportions maintain above r^2 values above 0.90 from the 2-4m cover level to the 32-64m cover level. The return

count r^2 values range from 0.32 to 0.47. The 25^{th} and 50^{th} percentile intensity metric r^2 values round to 0.00 and the 95^{th} percentile value rounds to 0.01. The structure class and rumple r^2 values are 0.94 and 0.92 respectively (Figure 8). The high R^2 value of the structure classes indicates the 13 stable input metrics produce stable output. Similarly, the high rumple R^2 value indicates the stable canopy surface models produce stable metrics after processing.

The unharvested area scatter plots show results similar to the overall area. The primary differences are less skew toward the 2010 acquisition in the 2-4m and 8-16m cover proportion metrics. The 95^{th} percentile intensity metric shows little correlation and the total return count plot shows decreasing correlation with increasing number of returns. The structure class and rumple distributions are more closely distributed around the 1:1 line and do not skew toward either acquisition (Figure 10).

The confusion matrix shows the structure class shifts over the unharvested area (Figure 12). The majority of classes remain constant, however there was some shift. There is no skew regarding an apparent increase or decrease in structure class estimation between the two years, suggesting the inconsistency is just noise between the acquisitions.

Harvested Area

The region that underwent harvesting between 2010 and 2012 was isolated and compared separately to determine how LiDAR metrics are influenced by structural changes in forest ecosystems. The average metric consistency is lower than the overall comparison (Table 3). The lower elevation return percentiles (p25) r^2 values decreased slightly more than the mid (p50), which decreased slightly more than the upper (p95): .05, .02, and .01 respectively. The cover proportion metrics however, display a more severe gradient. The lower cover metrics (represented by the proportion of canopy in the 2-4m range) drop by 0.40, the mid cover metrics (represented by the proportion of canopy in the 8-16m range) drop by 0.20) and the upper cover metrics (represented by the proportion of canopy in the 32-64m range) drop by

0.01. The return count r^2 values range from 0.40 to 0.56 and do not trend based on return number. The intensity metrics all round to 0.00 and do not trend based on percentile return. The structure class and rumple r^2 values drop by .03 and .09 respectively (Figure 8).

The harvested area scatter plots generally show a wider distribution of points associated with the lower r^2 values. Notable changes between the other comparisons include the strong skews toward the 2010 acquisition in the 2-4m and 8-16m cover proportion metrics. In addition, the 95th percentile elevation metric, the 32-64m metric, and the structure classes have outliers trending toward the 2010 acquisition. Conversely, the 25th percentile elevation metric is skewed toward the 2012 acquisition. The rumple metric is more evenly distributed. The total return count plot shows decreasing consistency with increasing number of returns and is skewed toward the 2012 acquisition. The 95th percentile intensity metric shows no correlation (Figure 11).

Different resolutions

Metric consistency is generally positively correlated with pixel size (among 15, 30, and 46 meters) (Figure 13). The cover metrics, elevation return percentages, total cover, elevation standard deviation, and elevation mean all display increasing r^2 values with increasing pixel size. The rumple r^2 value increases from 0.90 to 0.92 between 15 and 30 meter resolution, but decreases to 0.89 in the 46-meter resolution comparison. The structure class r^2 value decreases from 0.95 to 0.93 from the 30-meter resolution to the 46-meter resolution, and decreases to 0.89 in the 15-meter resolution. The 95th percentile intensity return shows no trend regarding pixel size. As these metrics are representatives, it is assumed these trends generally hold true for the full suite of metrics. Small deviations may occur however.

Dinkey2010 vs. Dinkey 2012 CSMs

The 1-meter CSM was compared over 4 segments. Block 1 has the smallest extent (9.1 acres) and has an R^2 value of 0.94 (Figure 14). Differences in a small area do not have a large spatial extent to average against, so some extreme changes due to anthropogenic alteration lower the R^2 value.

Block 2 covers 957.8 acres and has an R^2 value of 0.95 (Figure 14). Portions of the area experience minor height increases, but some areas experience height decreases up to 10 meters. The larger magnitude changes are infrequent and isolated.

Blocks 4 covers 1,508.0 acres and has an R^2 value of 0.96 (Figure 14). The maximum height difference in block 4 is a decrease of 6 meters, but most of the area does not experience any change. Larger magnitude changes occur in small and infrequent instances.

Block 5 is the largest extent, covering 6,306.5 acres. The r^2 value is 0.91, and the points are skewed toward the 2010 acquisition (Figure 14). There are frequent, low magnitude height increases throughout the area and infrequent, height decreases up to 15 meters. Block 5 contains the harvested area so we would expect a lower r^2 value due to tree removal. The map clip shows an example of the differences created from tree harvest (Figure 15).

Different resolutions

The R^2 value for the 1-meter resolution CSM extracted from block 2 is 0.96; the 2-meter CSM and 3-meter CSM R^2 values are both 0.95 (Figure 16).

Discussion

Previous LiDAR research has concluded there is a strong relationship between forest structure and the 25^{th} percentile return height, 95^{th} percentile return height, canopy proportion, and rumple. This study

focuses on these standard metrics, but includes intensity, return count, total cover, elevation standard deviation, and elevation mean consistencies to better represent the full suite of 204 metrics derived using FUSION.

The 2010 flight line comparisons showed that flight altitude (900-1500 meters), acquisition direction, and sensor type do not reduce LiDAR metric consistency. This stability allowed confident assessment of metric consistency between the 2010 and 2012 acquisitions despite the different acquisition specifications.

Structural change reflection

Metric comparisons over the harvest area provide insight into how metrics reflect structural changes in forest ecosystems. Scatter plots represent the point distributions around the $metric_{Dinkey2010} = metric_{Dinkey2012}$ line. Many of the representative metrics had slightly lower r^2 values in the harvested area, but the 2-4 meter cover proportion, the 8-16 meter cover proportion, and the rumple, decreased by a larger margin. The scatter plots for these lower canopy proportions show skew toward the 2010 acquisition, indicating the proportion of canopy in these strata layers was higher in 2010 than in 2012. This result is consistent with the Collaborative Forest Landscape Restoration Program Proposal, which outlines a fuel reduction management strategy consistent with the North et al. 2009 approach of reducing tree density and removing ladder fuels. This strategy focused on removing canopy in the 2-16 meter strata layers.

This revelation has implications for both ecosystem comparison and monitoring using aerial LiDAR. The derived cover metrics are very sensitive to structural change; they can be used to track whether management has met project goals and they can be used to determine if disturbances shift canopy strata weightings.

Note the harvest area is only 13% of the overall area, so it affects the overall comparison proportionately. This needs to be considered when investigating landscape changes. Taking overall comparison statistics of an area may not be representative of changes on smaller scales. The 2-4m difference map shows the extent of an area can be masked (Figure 17), but it is necessary to explore alternate methods such as examining difference maps to locate and determine the spatial extent of structural changes.

Metric consistency

Metric comparisons over the unharvested area are the best indicator for actual metric stability, as they exclude anthropogenic structural changes in the forest. The results of this comparison show the cover metrics, rumple, and elevation return percentiles above 25% will maintain r^2 values above 0.90; and the elevation mean, elevation standard deviation, and total cover above 2 meters have r^2 values above 0.95. As appendix 2 outlines, these metrics are used to derive the structural classes. The structure class r^2 value of 0.94 in the unharvested area implies the stable input yields a stable output.

The structure class stability between acquisitions is a key conclusion for forest researchers and managers as ecological forestry is largely built around altering the structure of a forest to more closely emulate natural conditions. These methods derive stable LiDAR structural classes, enabling both quantitative comparisons of forest characteristics over landscape-scales, and confidence that successive LiDAR acquisitions will be comparable with previous datasets.

The inconsistency of the intensity metrics has been discussed in previous studies (Goodwin et al. 2006, Bater et al. 2011). My results agree with these studies; intensity is unstable and should not be considered for monitoring or ecosystem comparison using LiDAR. Some vendors and manufacturers are, however, exploring methods to normalize intensity values. This would potentially increase consistency, allowing for accurate comparisons between acquisitions.

There is a general increase in r^2 value from the 30-meter resolution comparisons to the 46-meter comparisons, however high r^2 values are maintained in both. There is a discrepancy in 15-meter resolution comparisons however, with much lower consistency levels. Depending on the level of confidence necessary for a project, I suggest using a coarser processing resolution.

Canopy surface model

Canopy surface models are derived at a higher resolution, which enables structural changes to be identified down to the individual tree level. This allows for more specialized forest characteristics to be inspected. Some applications of interest include tracking individual tree growth and monitoring tree gap dynamics. Yu et al. (2004) for example, used canopy height models to successfully detect harvested and fallen trees, and to detect forest growth at plot and stand levels.

The high (R^2 >0.94) values for the canopy surface model comparisons indicate the models are consistent and can be compared between acquisitions. The high R^2 values are consistent with the results produced by Goodwin et al. (2006). They found the effect of flying altitudes, scan angles, and footprint sizes on LiDAR datasets do not have a major influence on canopy height models.

The outlier is block 5, with an R^2 value of 0.91. However, this lowered value is due to changes in the landscape, rather than inconsistencies in the LiDAR. This block contains tree height changes exceeding 40 meters as a result of the harvest. In this circumstance I hoped the R^2 value would be lower, indicating the canopy surface model reflects structural changes in the ecosystem.

The canopy surface model resolutions vary slightly with different resolutions, but maintain r^2 values above 0.95. Consistency does not have a trend regarding pixel size, suggesting stability between 1-3 meters should not be a factor when determining how to process canopy surface models.

Management Considerations

The fundamental finding of this study is that for many metrics repeat LiDAR measurements produce nearly similar results. Therefore, managers can use LiDAR metrics to measure the key height and canopy cover characteristics of their forest with confidence. However, repeat measurements show small variations indicating that there are limits to the precision of LiDAR metrics. Managers can trust that large differences in measurements reflect true differences in forest structure. However, small differences equal to a few percent of a measurement's value may reflect differences in measurement precision rather than real difference in forest structure.

Many metrics maintain consistency; however this study bolstered previous conclusions that intensity metrics are unstable. With our current level of technology intensity should not be considered consistent between acquisitions. Additionally, pulse return counts vary with flight altitude and should not be considered stable between acquisitions.

Overall, the high R^2 values found in this study show many metrics, as well as canopy surface models, can be compared over multiple acquisitions with confidence they are consistent. These tools will provide novel methods for ecosystem comparison, active management, and disturbance monitoring.

The planning, post-harvest, and long-term monitoring stages of active management will benefit from these results. For example, prior to an ecological harvest operation, a land manager can compare the characteristics of the stand of interest to a forest ecosystem with desirable structural characteristics. The canopy surface model will allow for fine-scale analyses such as determining tree clumping and gaps specifications and , the canopy proportion cover metrics can inform which strata layers need thinning, and the elevation return percentiles can provide estimation of current maximum tree heights (p95) and the height to live crowns (p25) in each ecosystem.

Following harvest, a manager can use LiDAR to confirm the desired structural characteristics were produced on individual tree scales and on landscape scales. On longer temporal scales, the canopy surface model can accurately provide individual tree height estimates and gap dynamics. The canopy proportion metrics can either confirm regeneration in each height strata is consistent with objectives, or isolate specifically what need further treatment.

Similarly, there are implications for disturbance quantification and monitoring. Wildfire is in a particularly concerning state due to fire suppression and extended droughts throughout western United States. If LiDAR data is available over an area before it burns, a direct comparison can be conducted to determine changes on individual tree, stand, or landscape scales between pre-fire and post-fire structural characteristics. If there is not pre-fire data, LiDAR can compare a burned area with adjacent, unaltered stands.

Long-term studies can be conducted over burned areas to follow mortality and regeneration trends following fires. Particularly when technology advances to the point where intensity metrics are consistent, researchers will be able to accurately identify mortality based on differences in canopy coloration. This will enable individual trees with scorching to be tracked and monitored to quantify survival rates following various levels of canopy damage.

These are a few examples of new opportunities given consistent LiDAR data. However, LiDAR has, and will continue to provide innovation regarding remote sensing in forestry, and technological advances will continue opening new doors.

Conclusion

This study demonstrates the applicability of using multiple LiDAR acquisitions to conduct ecosystem comparisons and monitoring. Determining which metrics are usable for a particular project depends on

desired standards; however we provide consistency levels for metrics and canopy surface models under a range of conditions.

The consistency of metrics is not reduced by flying altitude (between 1100 and 1500 meters), sensor model, or flight direction. In addition, the cover metrics, rumple, and elevation return percentiles above 25% will maintain r^2 values above 0.90; and the elevation mean, elevation standard deviation, and total cover > 2 meters have r^2 values above 0.95. R^2 values are generally positively correlated with absolute (meter) and relative (percentile) height in canopy. 30- and 46-meter pixel sizes maintain high correlation, but consistency deteriorates using a 15-meter resolution.

Cover proportion metrics strongly reflect structural changes in the forest. In this study, cover values in the 2-4- and 8-16-meter height stratas were influenced by thinning operations.

Canopy surface model consistency varies, but maintains r^2 values above 0.95 for pixel sizes ranging 1-3 meters.

References Cited:

Bater, C. W., Wulder, M. A., Coops, N. C., Nelson, R. F., Hikler, T., & Næsset, E. 2011. Stability of sample-based scanning-LiDAR-derived vegetation metrics for forest monitoring. IEEE Transactions on Geoscience and Remote Sensing, 49, 2385–2392.

Department of Geology and Mineral Industries. 2013. Alaska DNR LiDAR Project, 2012 - Whittier Acceptance Report.

Dinkey Creek Planning Forum. 2010. Collaborative Forest Landscape Restoration Program Proposal. Sierra National Forest Pacific Southwest Region.

Fekety, P. A., falkowski, M. J., Hudak, A. T. 2014. Temporal transferability of LiDAR-based imputation of forest inventory attributes. *Canadian Journal of Forest Research*, 10.1139.

Franklin, J.F., and Spies, T.A. 1991. Composition, function, and structure of old-growth Douglas-fir forests. In Wildlife and vegetation of unmanaged Douglas-fir forests. Edited by L.F. Ruggiero, K.B. Aubry, A.B. Carey, and M.H. Huff. U.S. For. Serv. Gen. Tech. Rep. PNW-GTR-285. pp. 71–80.

Gobakken, T. and Næsset, E. "Assessing effects of laser point density, ground sampling intensity, and field sample plot size on biophysical stand properties derived from airborne laser scanner data," *Can. J. Forest Res.*, vol. 38, no. 5, pp. 1095–1109, May 2008.

Goodwin, N. R., Coops, N. C., and Culvenor, D. S. 2006. "Assessment of forest structure with airborne LiDAR and the effects of platform altitude," *Remote Sens. Environ.*, vol. 103, no. 2, pp. 140–152.

Holmgren, J., Nilsson, M., & Olsson, H. (2003). Simulating the effects of lidar scanning angle for estimation of mean tree height and canopy closure. Canadian Journal of Remote Sensing, 29(5), 623−632.

Hopkinson, C., (2006). The influence of lidar acquisition settings on canopy penetration and laser pulse return characteristics. Proceedings of the joint IGARSS and CSRS meeting held in Denver, Colorado, July 2006. Published on CDROM by the Geosciences and Remote Sensing Society (unpaginated).

Hopkinson, C., Chasmer, L, and Hall, R. J. 2007. The uncertainty in conifer plantation growth prediction from multi-temporal lidar datasets. Remote Sensing of Environment 112:1168-1180. doi:10.1016/j.rse.2007.07.020.

Hopkinson, C. 2007. "The influence of flying altitude, beam divergence, and pulse repetition frequency on laser pulse return intensity and canopy frequency distribution," *Can. J. Remote. Sens.*, vol. 33, no. 4, pp. 312–324.

Hudak, A.T., Strand, E.K., Vierling, L.A., Byrne, J.C., Eitel, J.U.H., Martinuzzi, S., Falkowski, M.J. 2012. Quantifying aboveground forest carbon pools and fluxes from repeat LiDAR surveys. Remote Sensing of Environment 123:25-40. doi:10.1016/j.rse.2012.02.023.

Kane, V.R., McGaughey, R.J., Bakker, J.D., Gersonde, R.F., Lutz, J. A., and Franklin, J.F. 2010a. Comparisons between field- and LiDAR-based measures of stand structural complexity. Can. J. For. Res. 40(4): 761–773. doi:10.1139/X10-024.

Kane, V.R., Bakker, J.D., McGaughey, R.J., Lutz, J.A., Gersonde, R. F., and Franklin, J.F. 2010b. Examining conifer canopy structural complexity across forest ages and elevations with LiDAR data. Can. J. For. Res. 40(4): 774–787. doi:10.1139/X10-064.

Kane, V. R., Gersonde, R. F., Lutz, J. A., McGaughey, R. J., Bakker, J.D., & Franklin, J. F. 2011. Patch dynamics and the development of structural and spatial heterogeneity in Pacific Northwest forests. Canadian Journal of Forest Research, 41, 2276–2291.

Kane, V. R., Lutz, J. A., Roberts, S. L., Smith, D. F., McGaughey, R. J., Povak, N. A., et al. 2013. Landscape-scale effects of fire severity onmixed-conifer and red fir forest structure in Yosemite National Park. Forest Ecology and Management, 287, 17–31.

Lefsky, M.A., Hudak, A.T., Cohen, W.B., and Acker, S.A. 2005. Geographic variability in lidar predictions of forest stand structure in the Pacific Northwest. Remote Sens. Environ. 95(4): 532–548. doi:10.1016/j.rse.2005.01.010.

Legendre, P., and Legendre, L. 1998. Numerical ecology. 2nd English edition. Elsevier Science BV, Amsterdam, The Netherlands.

Lindenmayer, D.B., and Franklin, J.F. 2002. Conserving forest biodiversity: a comprehensive multi-scaled approach. Island Press, Washington, D.C.

Magnusson, M. , Fransson, J. E. S., and Holmgren, J. “Effects on estimation accuracy of forest variables using different pulse density of laser data,” *Forest Sci.*, vol. 53, no. 6, pp. 619–626, Dec. 2007.\

McCune, B., and Grace, J.B. 2002. Analysis of ecological communities. MjM Software Design, Gleneden Beach, Ore.

McElhinny, C., Gibbons, P., Brack, C., and Bauhus, J. 2005. Forest and woodland stand structural complexity: its definition and measurement. For. Ecol. Manag. **218**(1–3): 1–24. doi:10.1016/j. foreco.2005.08.034.

McGaughey, R. 2014. FUSION/LDV: Software for LiDAR data analysis and visualization. PDF. June 10, 2015. <http://forsys.cfr.washington.edu/fusion/FUSION_manual.pdf>

Means, J. E., Acker, S. A., Fitt, B. J., Renslow, M., Emerson, L., Hendrix, C. J. 2000. Predicting forest stand characteristics with airborne scanning LiDAR. Photogrammetric Engineering & Remote Sensing Vol. 66, No. 11, pp. 1367-1371.

Næsset, E. 2004. "Effects of different flying altitudes on biophysical stand properties estimated from canopy height and density measured with a small footprint airborne scanning laser," *Remote Sens. Environ.*, vol. 91, no. 2, pp. 243–255.

Næsset, E., & Gobakken, T. 2005. Estimating forest growth using canopy metrics derived from airborne laser scanner data. Remote Sensing of Environment, 96, 453−465.

Næsset, E. 2005. "Assessing sensor effects and effects of leaf-off and leaf-on canopy conditions on biophysical stand properties derived from small footprint airborne laser data," *Remote Sens. Environ.*, vol. 98, no. 2/3, pp. 356–370.

Oksanen, J., Blanchet, F. G., Kindt, R., Legendre, P., Minchin, P. R., O'Hara, R. B., Simpson, G. L., Solymos, P., Henry, M., Stevens, H., Wagner, H. 2015. Community Ecology R Package, 'vegan'. R Version 2.3-0.

Reutebuch, S. E., Anderson, H. E., McGaughey, R. J., Carson, W. W. 2003. Accuracy of a high-resolution lidar terrain model under a conifer forest canopy. Can. J. Remote Sensing, Vol. 29, No. 5, pp. 527 – 535.

Reutebuch, S. E., Anderson, H. E., McGaughey, R. J. 2005. Light Detection and Ranging (LiDAR): An Emerging Tool for Multiple Resource Inventory. Journal of Forestry.

Spies, T.A. 1998. Forest structure: a key to the ecosystem. Northwest Sci. 72: 34–39.

St-Onge, B., and Vepakomma, U. 2004. Assessing forest gap dynamics and growth using multi-temporal laser-scanner data, *International Archives of Photogrammetry, Remote Sensing and Spatial Information Sciences*, 03–06 October, Freiburg, Germany, Institute for Forest Growth, Department of Remote Sensing and Landscape Information Systems, University of Freiburg, Freiburg, Germany, Vol. XXXVI, Part 8/W2, pp. 173–178.

Sweda, T., Tsuzuki, H., Kusakabe, T. (2003). Climate-induced vegetation change in Canadian boreal forest as detected by airborne laser profiling. In J. Hyyppa¨, E. Næsset, H. Olsson, T. Granquist Palen, & H. Reese (Eds.), Scandlaser scientific workshop on airborne laser scanning of forests. Working Paper, Vol. 112. (pp. 108 – 114). Umea˚, Sweden' Swedish University of Agricultural Sciences, Department of Forest Resource Management and Geomatics.

Yu, X., Hyyppä, J, Kaartinen, H, and Maltamo, M. 2004. Automatic detection of harvested trees and determination of forest growth using airborne laser scanning, *Remote Sensing of Environment*, 90:451–462.

Yu, X., Hyyppä, J., Kukko, A., Maltamo, M., and Kaartinen, H. 2006. Change detection techniques for canopy height growth measurements using airborne laser scanner data. Photogrammetric Engineering and Remote Sensing. 72(12):1339-1348.

Figures

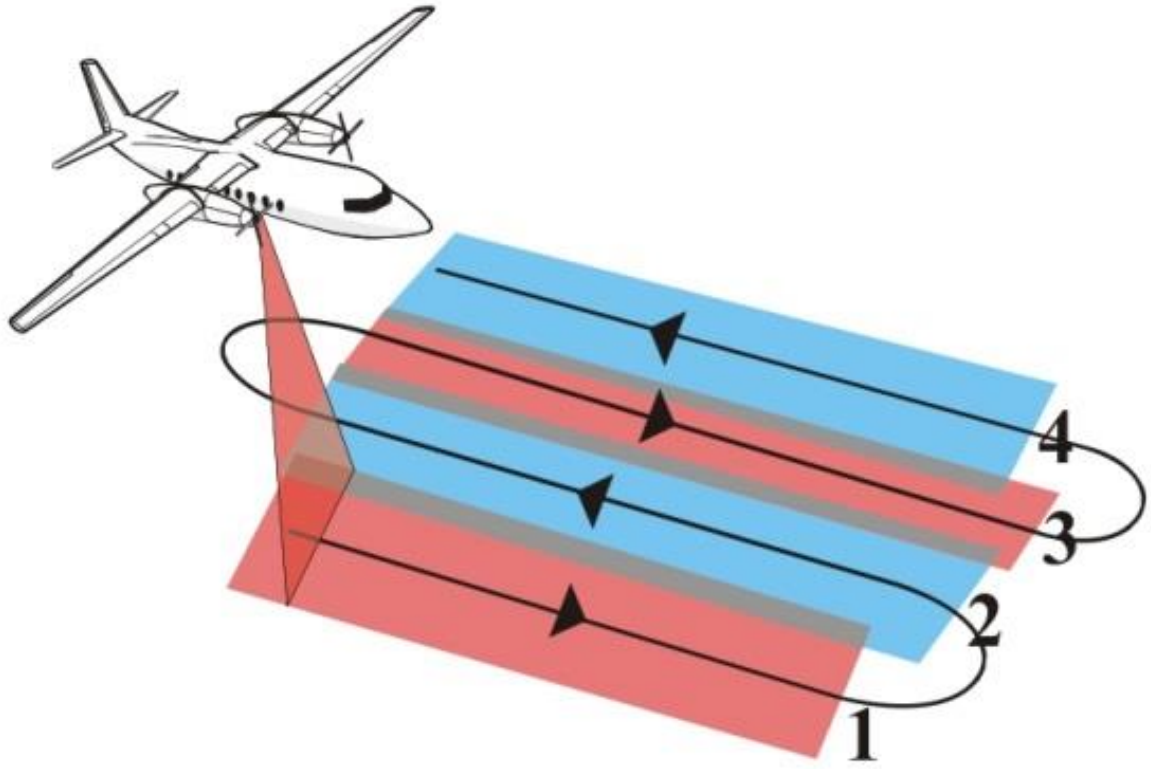

Figure 1: Flight lines 1, 2, 3, and 4 (left) contain overlap to minimize the possibility of having gaps in datasets. Points in the overlapping areas represent data from different acquisition specifications, allowing for multiple levels of comparison.

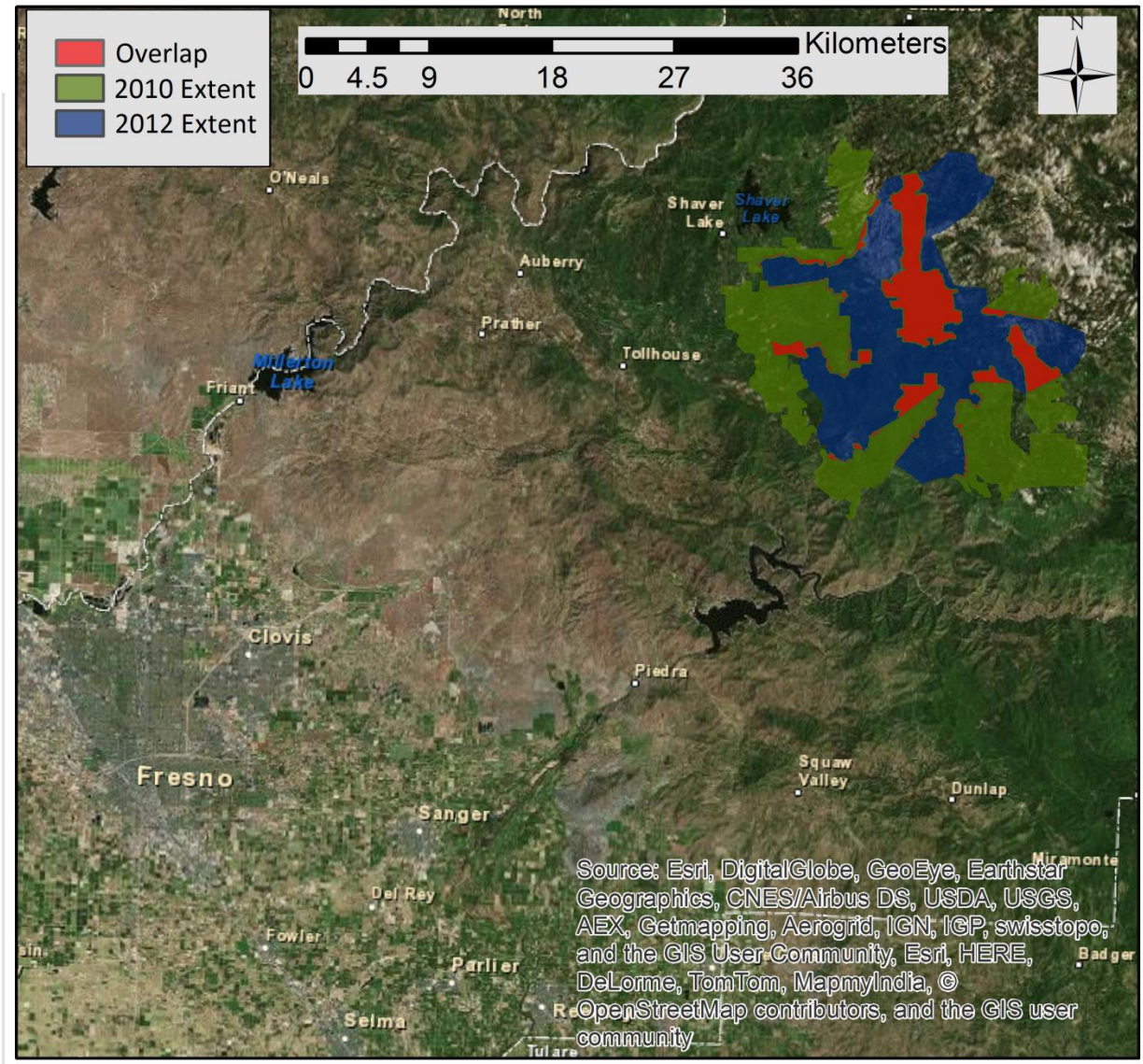

Figure 2: Map of the Dinkey LiDAR acquisitions, shown in relation to Fresno, California to provide context. The blue represents the 2010 acquisitions and the green represents the 2012 acquisition. The overlapping areas, buffered by 100m, are represented by red.

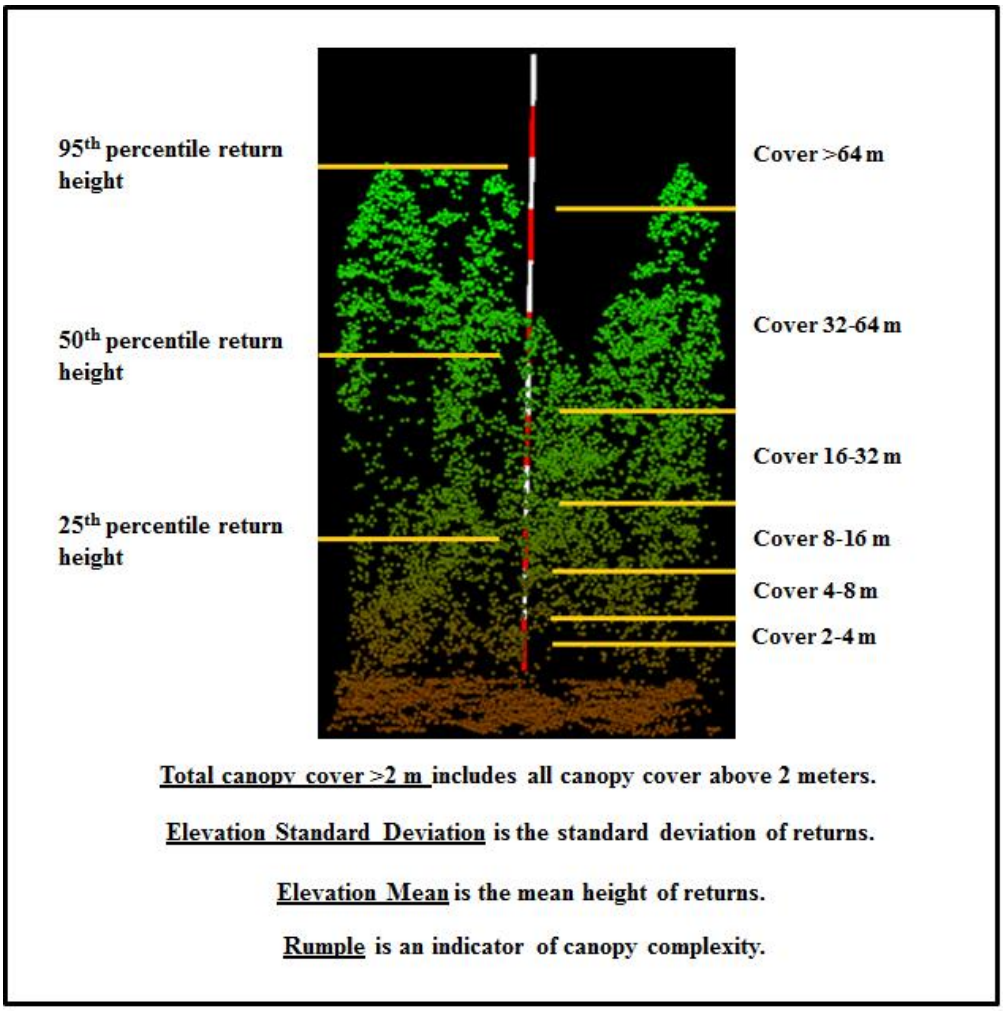

Figure 3: Metrics used to define the structural classes.

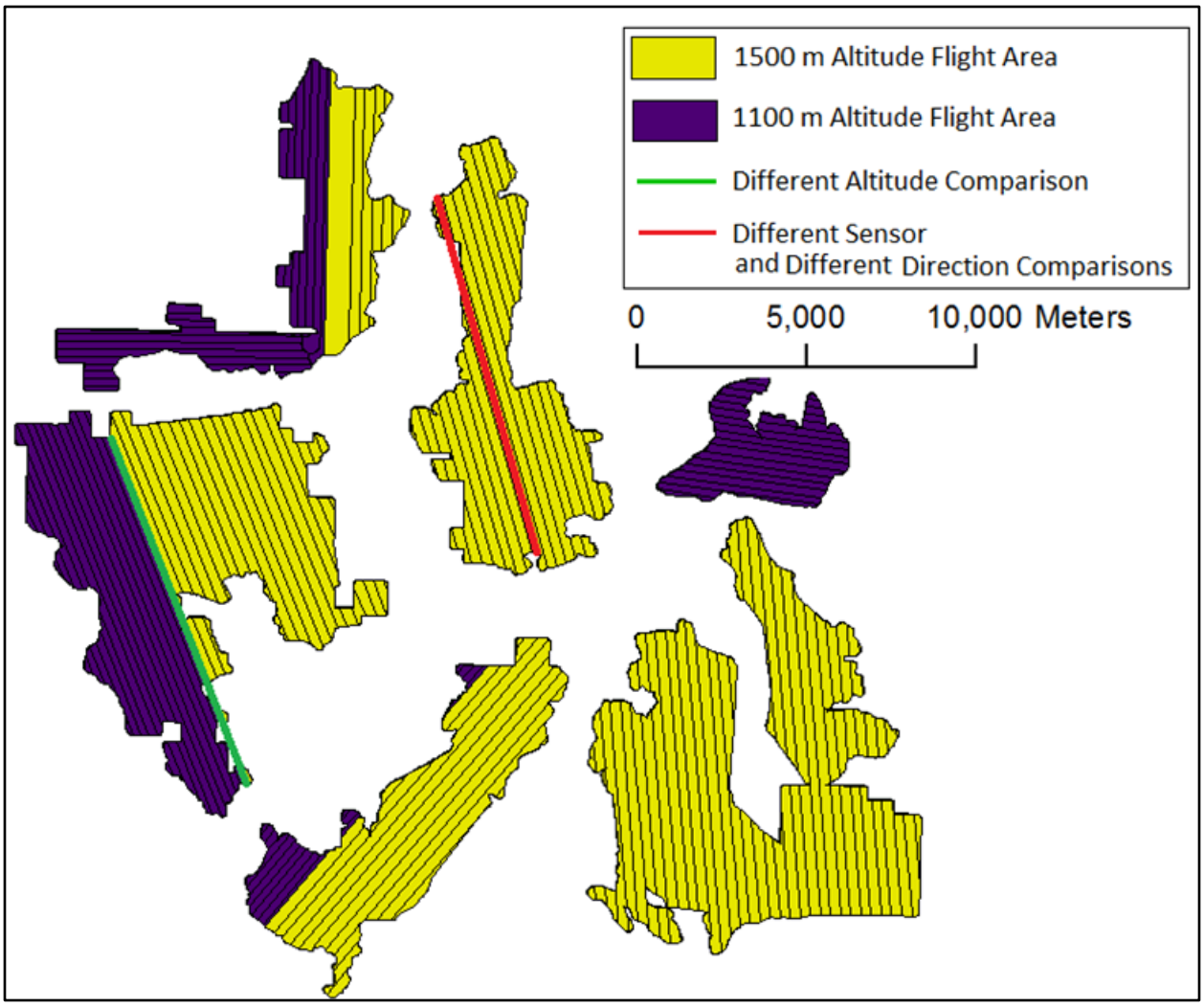

Figure 4: Map of the Dinkey Creek 2010 acquisition. Data was collected at two elevations: 1100 m (purple) and 1500 m (yellow). The intra-acquisition comparisons include: the area between flight lines of the same flight altitude (red), and flight lines between flight lines of different altitudes (green).

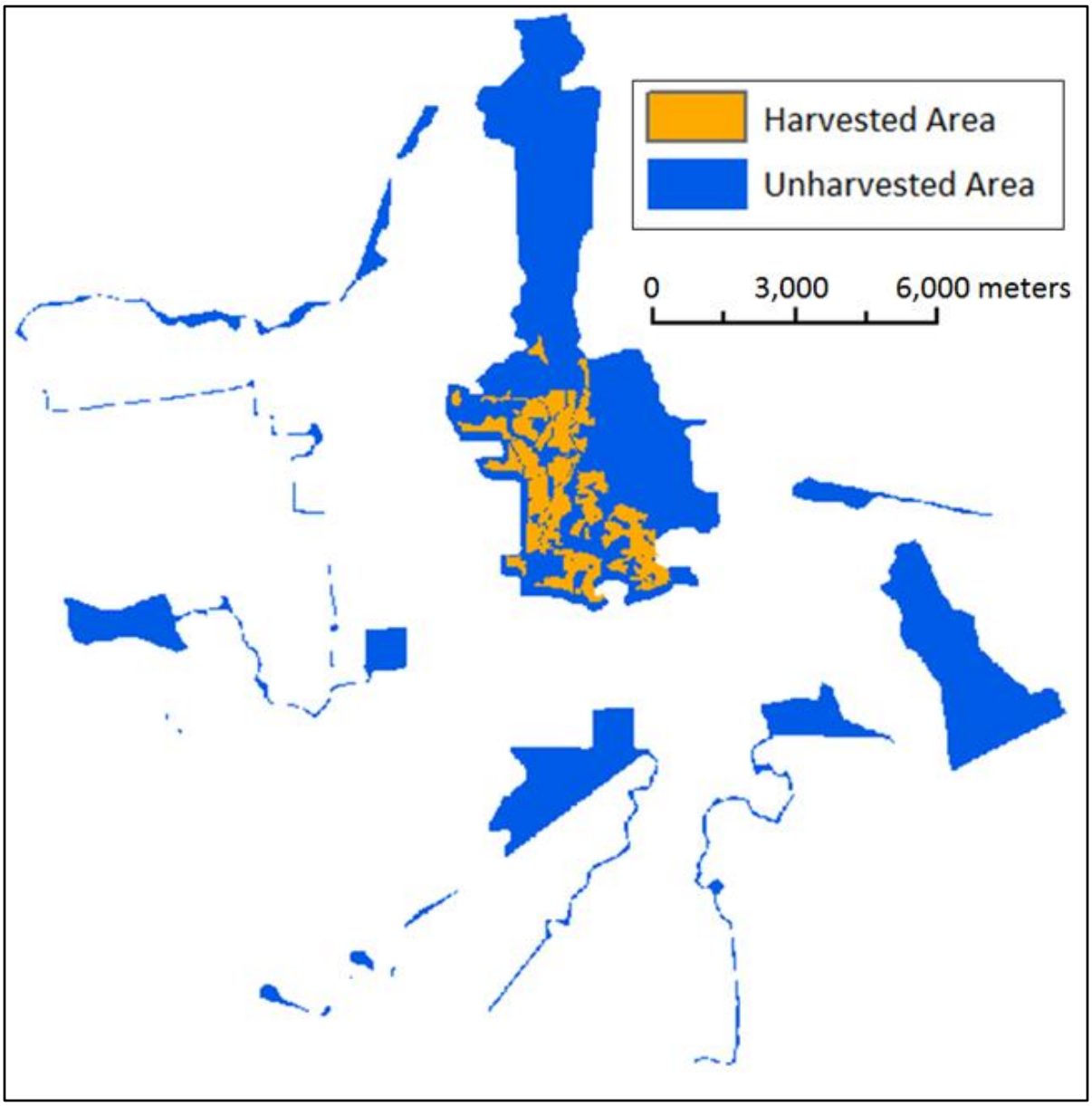

Figure 5: Map of the Dinkey Creek 2010:2012 overlap. Active management conducted between the acquisitions is indicated in blue. Comparisons were conducted for the overall area, the harvested area, and the unharvested area.

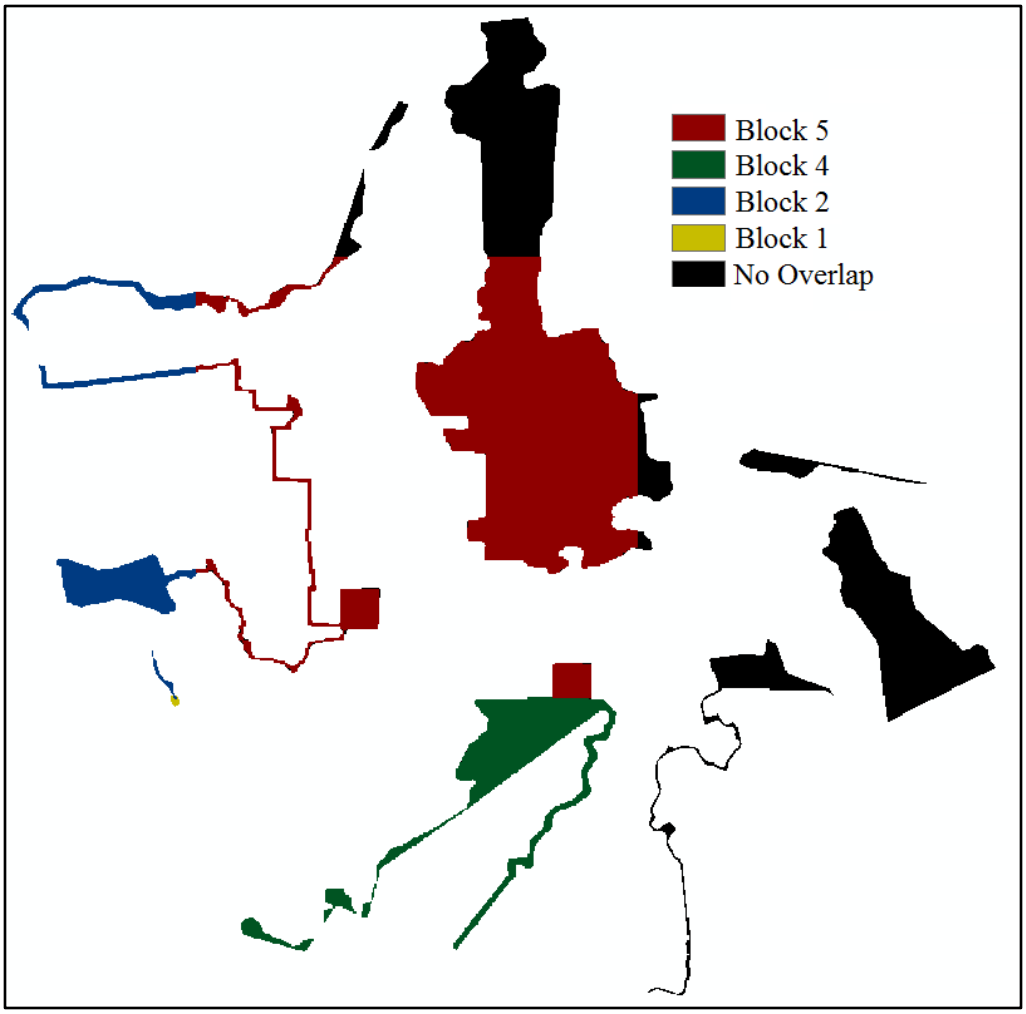

Figure 6: Blocks used for processing and comparing the canopy surface models.

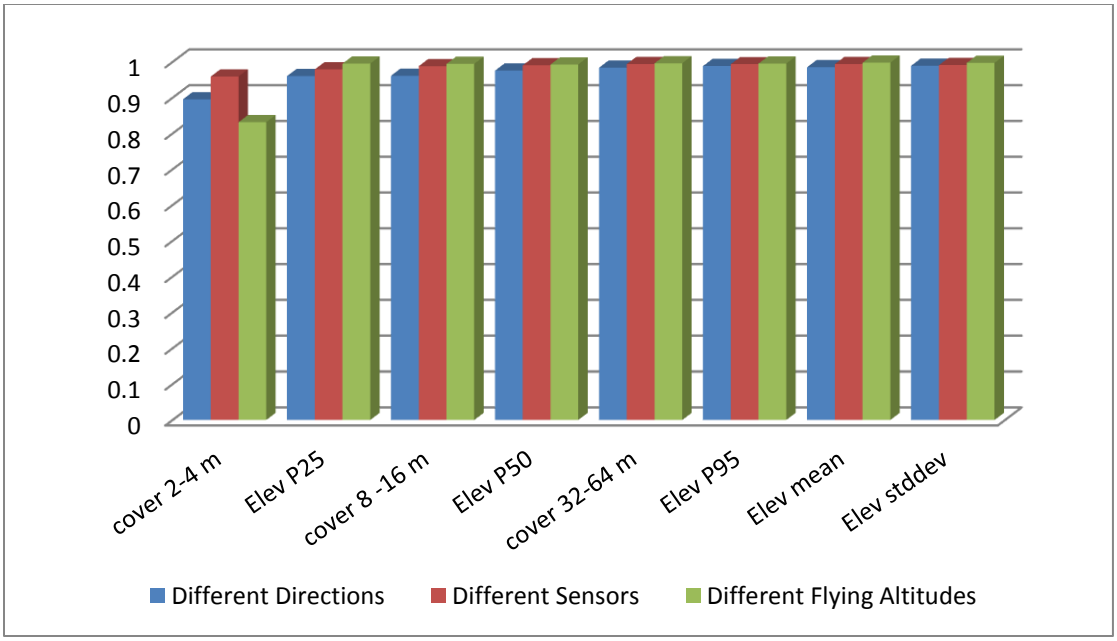

Figure 7: Histogram showing the R^2 value for flight Line 106:107 (different directions), flight line 106:1109 (different sensors), and flight line 39:75 (different flying altitudes) of the elevation metrics and the the canopy proportion(cover) metrics.

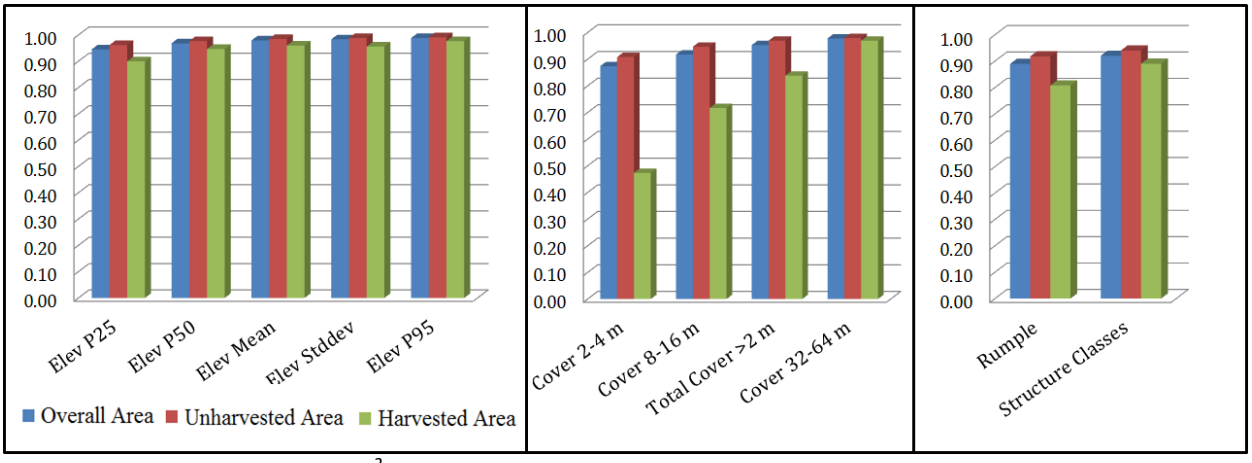

Figure 8: Histogram showing the R^2 value for the Dinkey 2010:Dinkey 2012 comparisons. Included are the elevation metrics (left), the cover proportions (middle), and the rumple and structure classes (right).

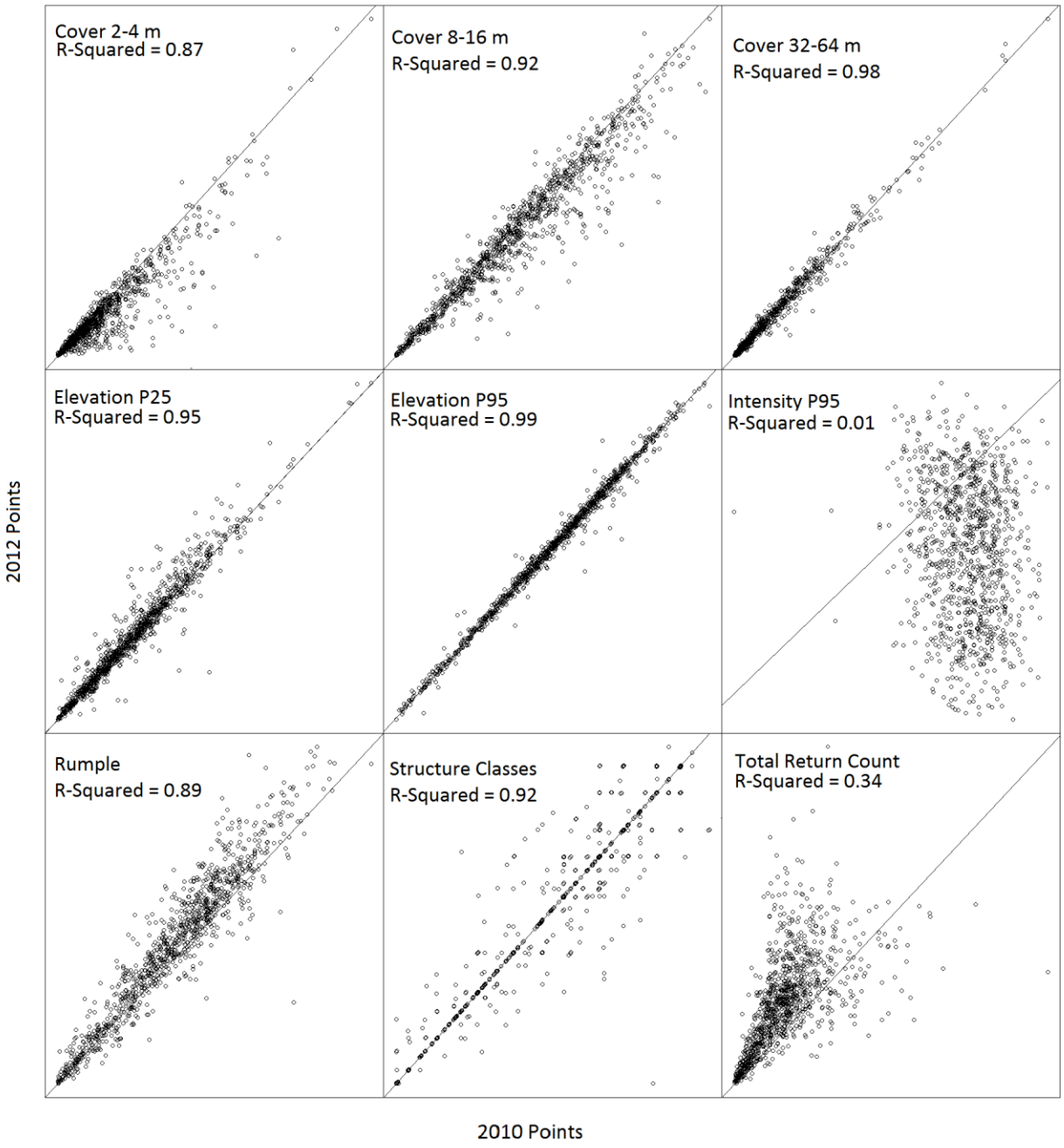

Figure 9: Scatter plots of the representative metrics of the entire overlapping area. Intensity p25 and p50, as well as return counts 1-4 are omitted because the consistencies are similar, and can be represented by the intensity p95 and total return count respectively. Units are not included because we are interested in the relationships between, not the absolute values of, the points. ADD STDDEV AND TOTAL COVER > 2

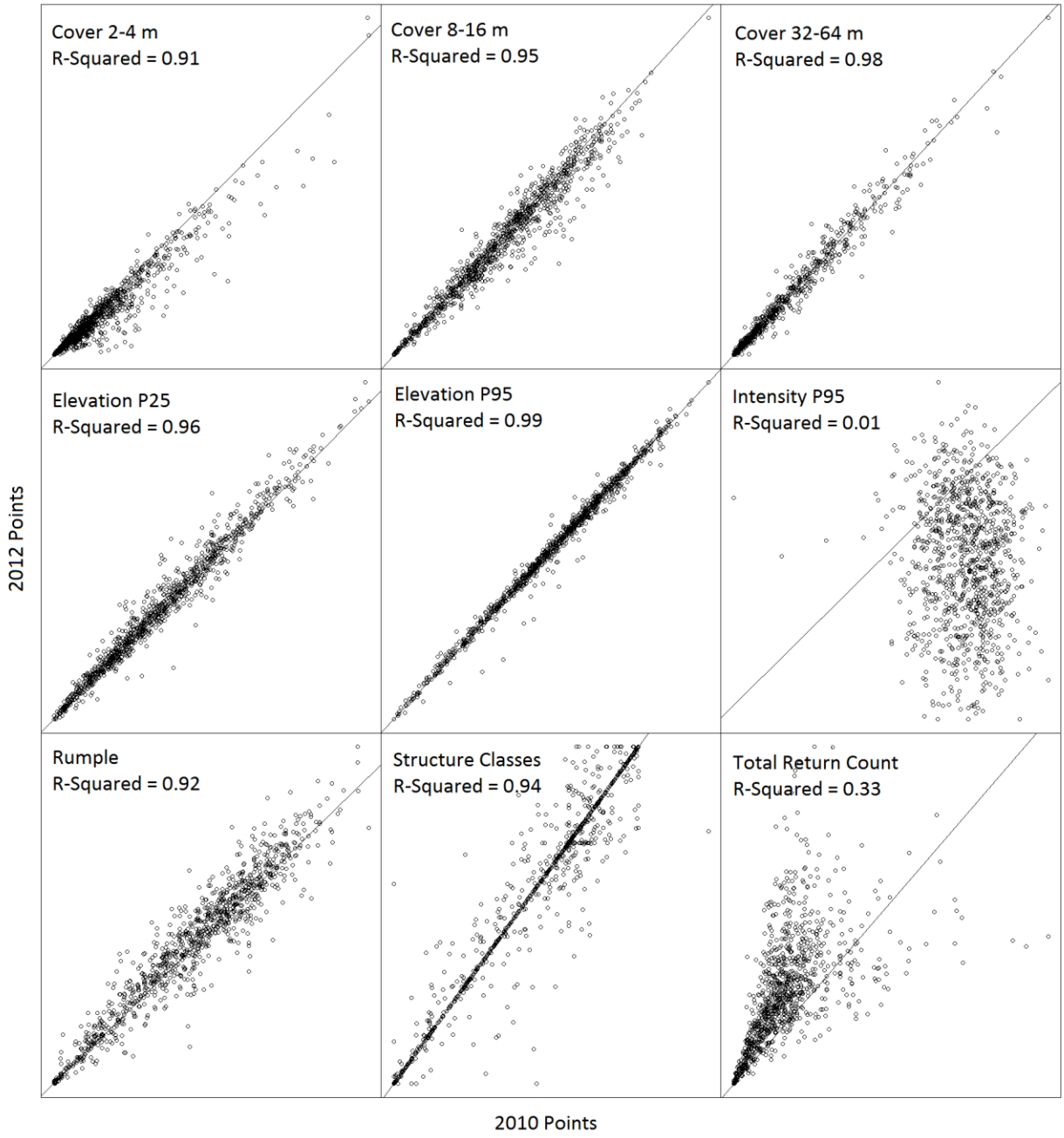

Figure 10: Scatter plots of the representative metrics of the unharvested area. Intensity p25 and p50, as well as return counts 1-4 are omitted because the consistencies are similar, and can be represented by the intensity p95 and total return count respectively. Units are not included in each plot because we are interested in the relationships between, not the absolute values of, the points. ADD STDDEV AND TOTAL COVER > 2

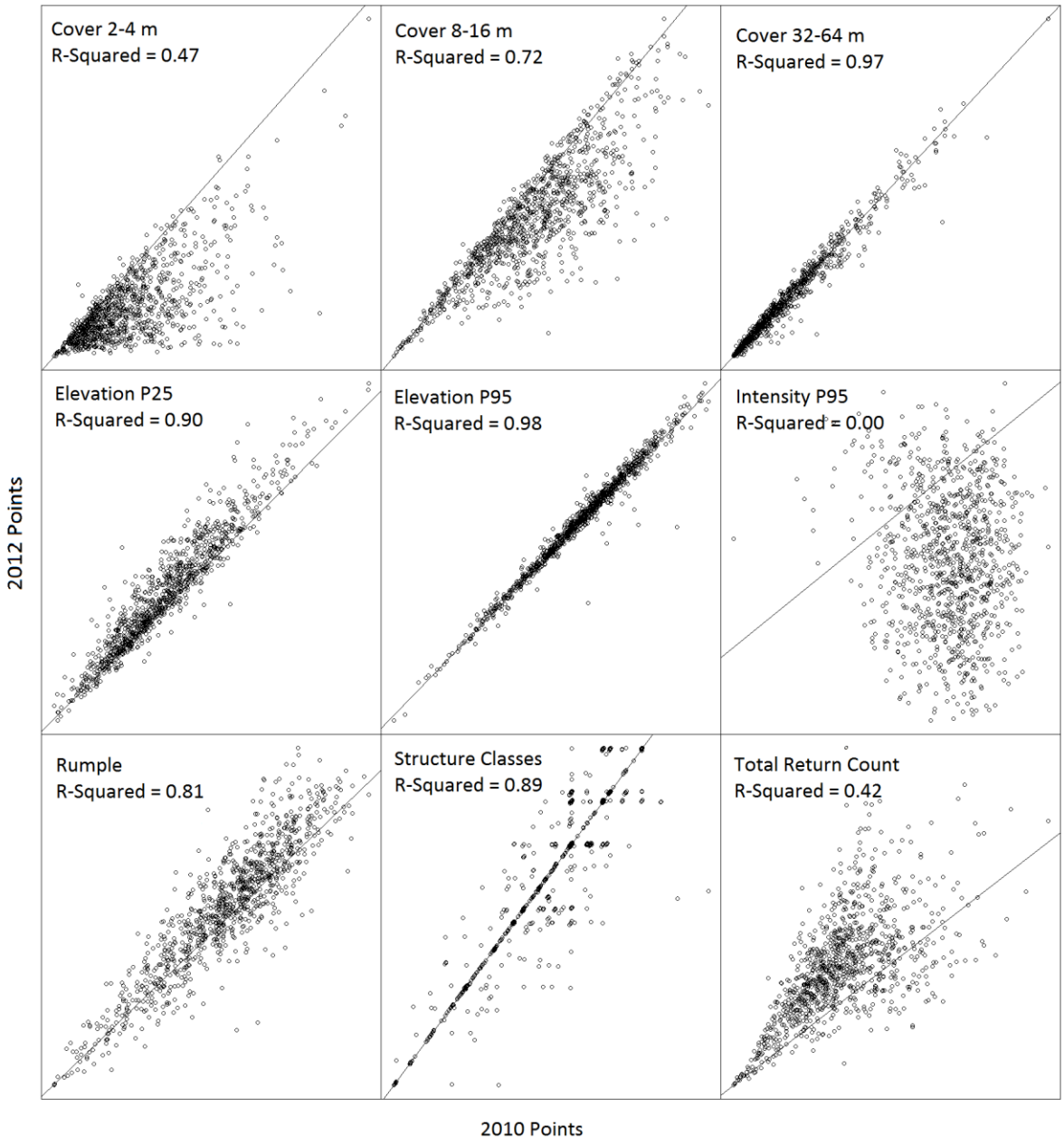

Figure 11: Scatter plots of the representative metrics of the harvested area. Intensity p25 and p50, as well as return counts 1-4 are omitted because the consistencies are similar, and can be represented by the intensity p95 and total return count respectively. Units are not included because we are interested in the relationships between, not the absolute values of, the points. ADD STDDEV AND TOTAL COVER > 2

	1	2	3	4	5	6	7	8	9
1	**0.94**	0.06	0.00	0.00	0.00	0.00	0.00	0.00	0.00
2	0.04	**0.80**	0.11	0.01	0.00	0.00	0.00	0.00	0.00
3	0.01	0.11	**0.77**	0.10	0.02	0.01	0.00	0.00	0.00
4	0.00	0.02	0.08	**0.74**	0.07	0.01	0.00	0.00	0.00
5	0.00	0.01	0.02	0.11	**0.75**	0.06	0.01	0.00	0.00
6	0.00	0.00	0.01	0.03	0.13	**0.86**	0.14	0.04	0.00
7	0.00	0.00	0.00	0.00	0.02	0.06	**0.81**	0.21	0.00
8	0.00	0.00	0.00	0.00	0.00	0.00	0.03	**0.75**	0.00
9	0.00	0.00	0.00	0.00	0.00	0.00	0.00	0.00	**1.00**

Figure 12: Confusion matrix showing the proportion of structure classes that remained consistent or shifted throughout the unharvested area between 2010 (x-axis) and 2012 (y-axis).

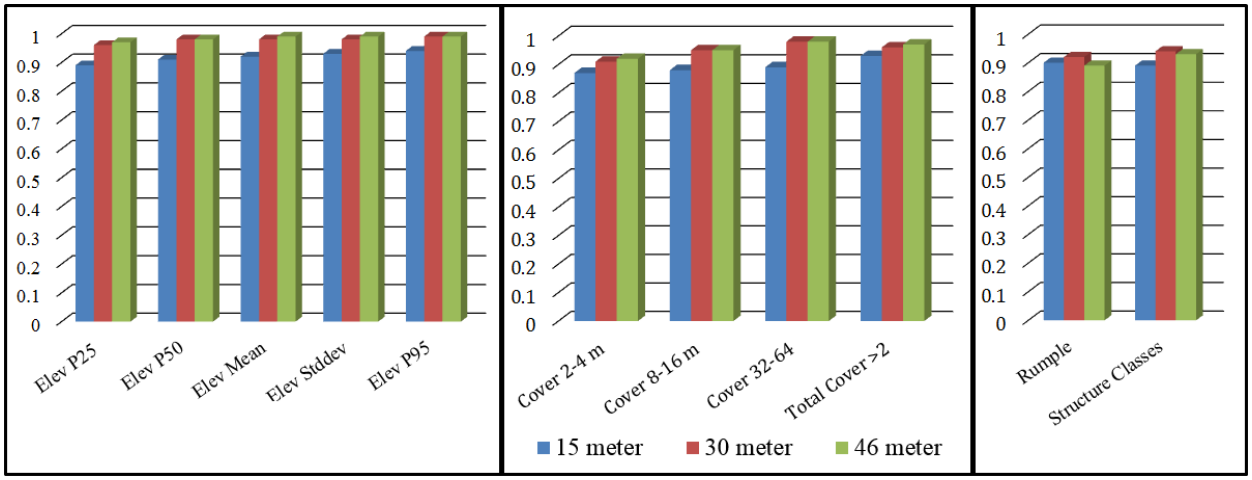

Figure 13: R^2 histograms of the 15-, 30-, and 46-meter resolutions calculated over the unharvested area of the Dinkey Creek Watershed. Included are the elevation metrics (left), the cover proportions (middle), and the rumple and structure classes (right).

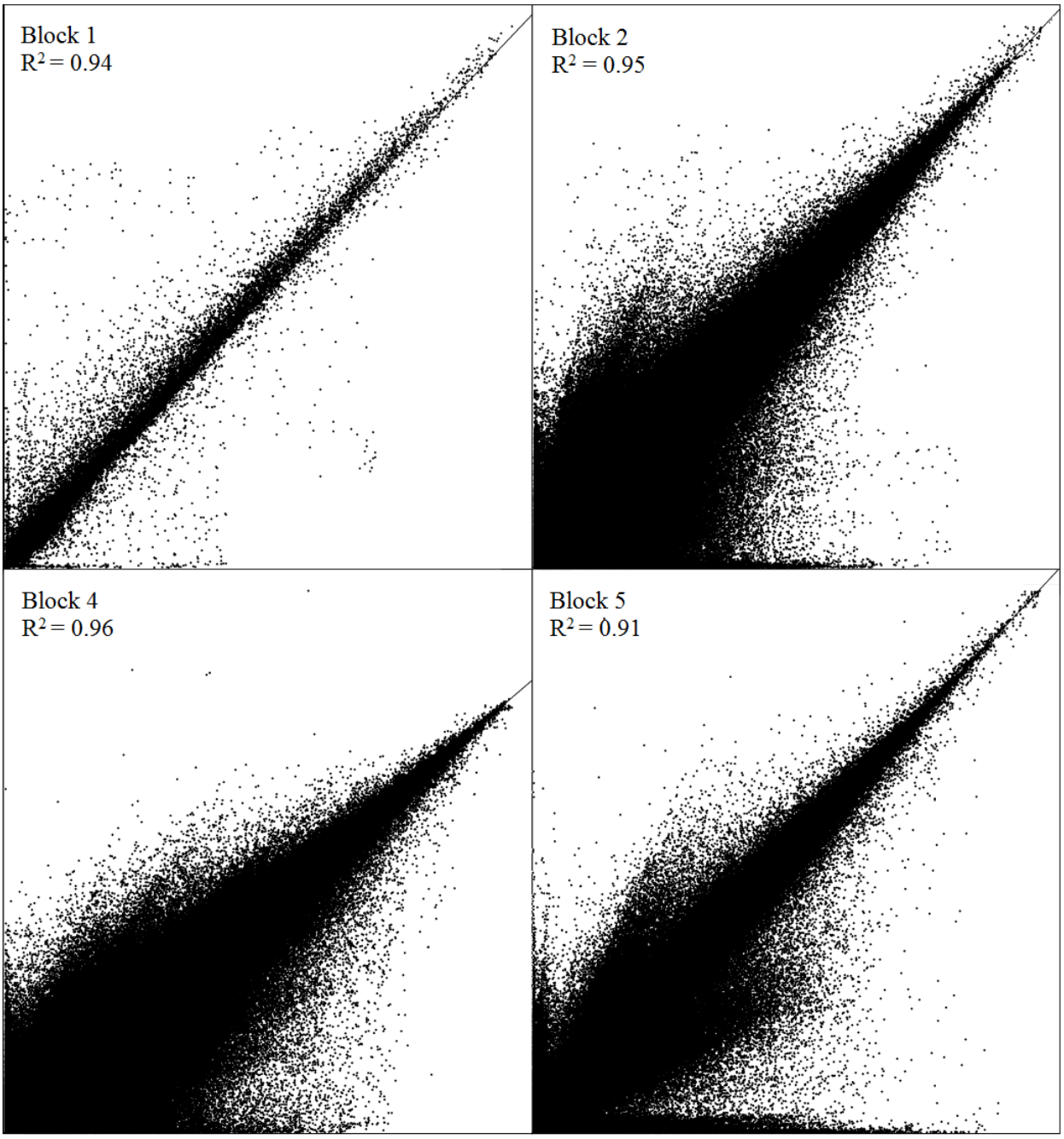

Figure 14: Scatter plots and R^2 values for the canopy surface model comparisons.

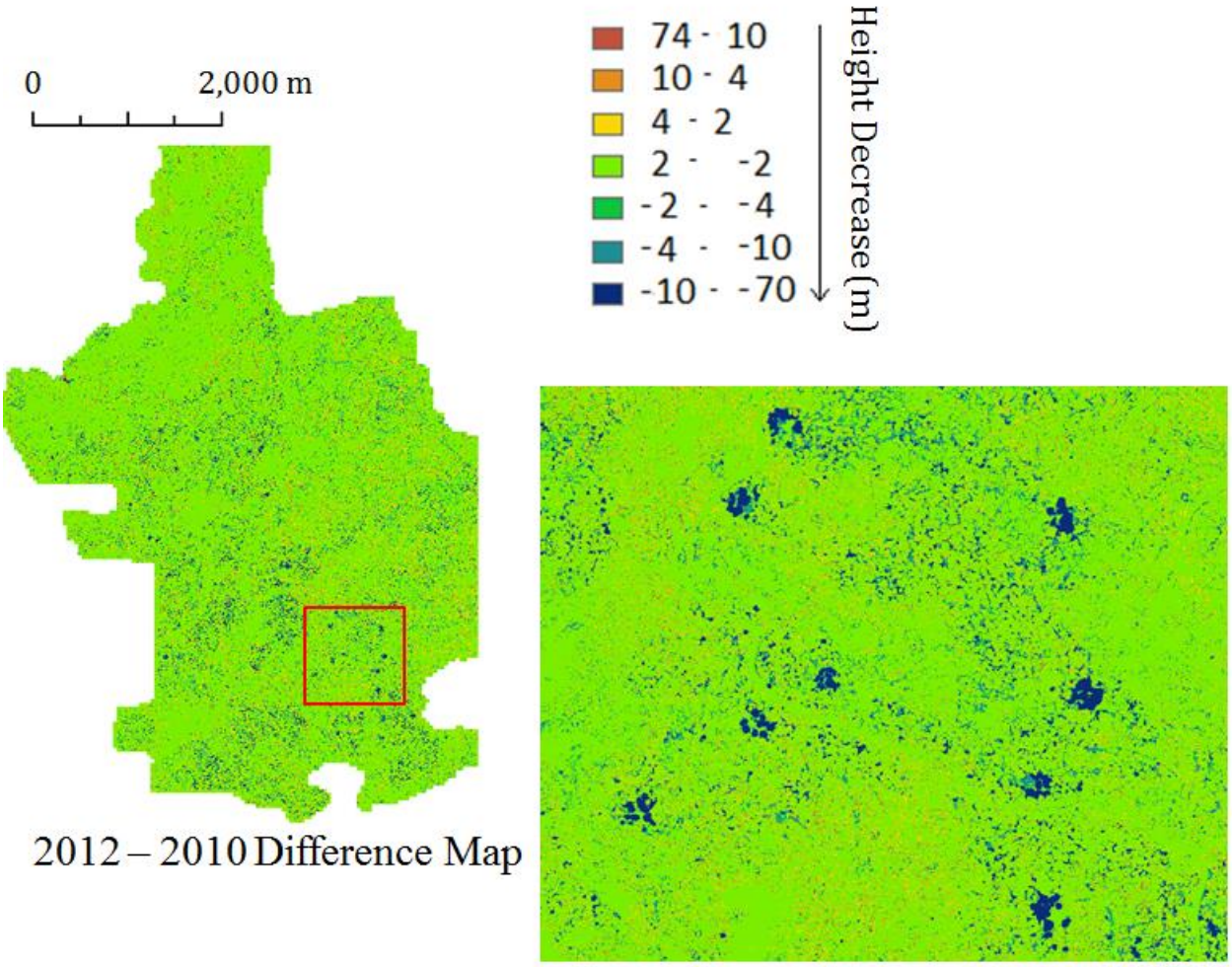

Figure 15: Reflection of timber harvest in the canopy surface model. Note the largely consistent (change between -2 and +2 meters) distribution of points. Also note however, harvest operations are apparent, represented by large decreases in canopy height between 2010 and 2012.

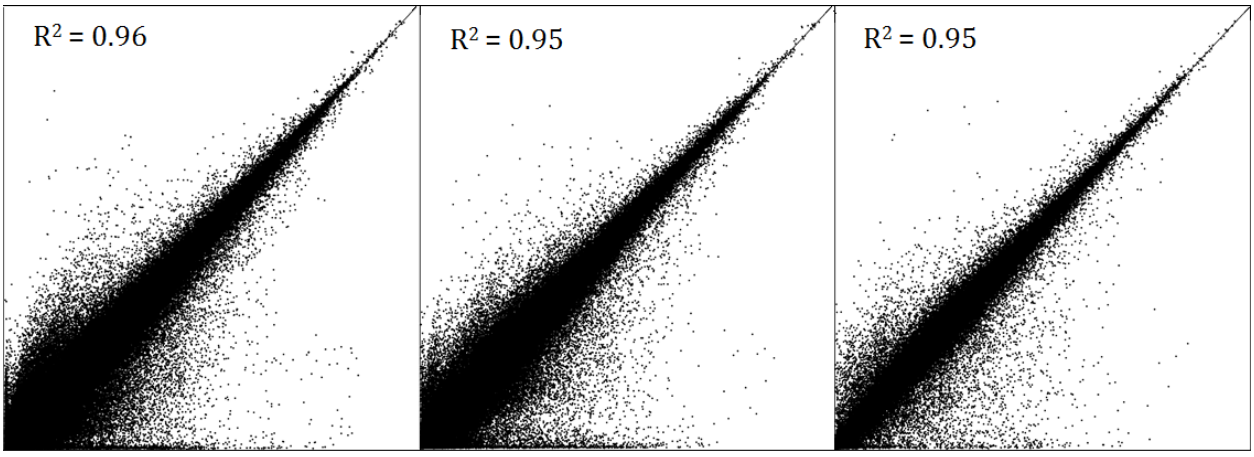

Figure 16: Canopy surface model comparisons among 1-meter resolution (left), 2-meter resolution (middle), and 3-meter resolution (right) canopy surface models over a 1,000 m^2 segment of block 2.

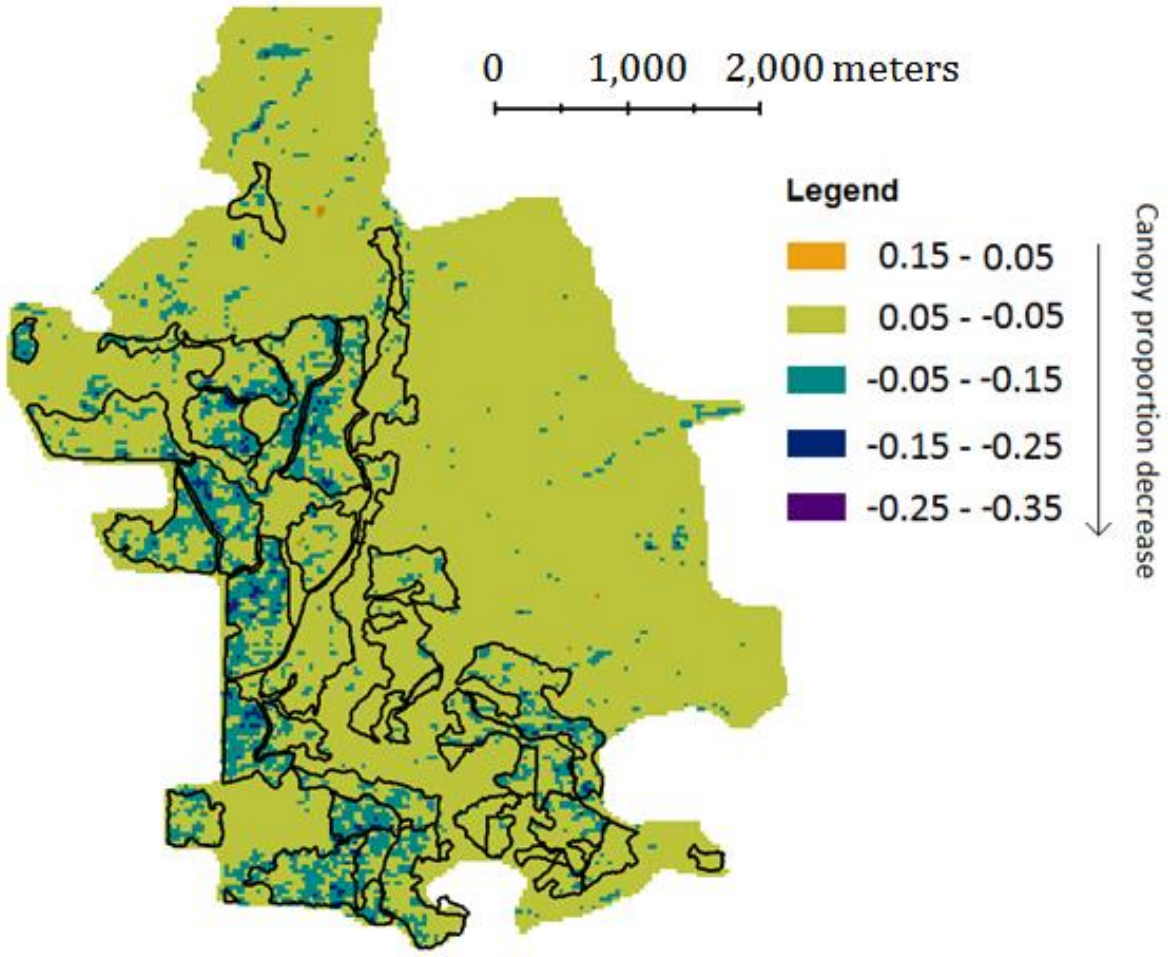

Figure 17: Difference map showing the cover decrease in the 2-4-meter strata layer.

Tables

Table 1: Regression coefficients used to compare ground models.

Coefficients				
	Estimate	Standard Error	t-value	p-value
Intercept	5.33e-2	5.15e-2	1.04	0.3
Slope	1.00e0	2.75e-5	36,306.03	2.00e-16
Multiple R^2	1.00	Adjusted R^2	1.00	

Table 2: R^2value summary statistics for all flight line metrics.

Comparison	**% of metrics with R^2 values above:**		
	0.90	**0.75**	**0.50**
Different Directions	29.4	52.4	77.1
Different Sensors	39.4	61.8	76.5
Different Altitudes	48.0	75.7	79.6

Table 3: R^2 value summary statistics for all Dinkey 2010:Dinkey 2012 metrics.

Comparison	**% of metrics with R^2 values above:**		
	0.90	**0.75**	**0.50**
Overall Area	30.2	44.1	56.9
Non-harvested Area	34.9	47.2	59.6
Harvested Area	20.7	37.4	55.2

Appendices

Appendix 1: Products delivered

Watershed Sciences created multiple products from the raw Dinkey 2010 LiDAR data for the USDA Forest Service. These deliverables include Smoothed Best Estimate of Trajectory (SBET) files in ascii and shapefile format; 1-meter resolution bare earth ground model in ESRI GRID format; 1-meter CSM in ESRI GRID format; all return point data in *.las version 1.2 format and ascii formats; Ground Classified Points in ascii format, 1/2 –meter resolution intensity images in GeoTIFF format; shapefiles of delivery area in 0.75 USGS QUAD, 7.5 USGS Quad, and study area; data report summarizing data acquisition, processing, and summary statistics; FDGC compliant metadata; Poster image of study area; and a shapefile or flighline centerline and swath edges.

Watershed Sciences Inc. created multiple products from the raw Dinkey 2012 LiDAR data for the USDA Forest Service. These deliverables include LAS files for all returns; 1-meter Bare Earth and Highest Hit Models; 1-meter resolution intensity images. Shapefiles provided by the vendor include site boundary, LiDAR index, DEM/DSM index, Smooth Best Estimate Trajectory (SBETs), flight lines, flight swaths, and ground point maps.

Appendix 2: structure class characteristics

The bar plots display the relationships between the structural classes and the LiDAR metrics, providing a fundamental understanding of structural class characteristics. The structure classes are ordered by the 95th percentile return height, meaning class 1 contains the shortest structures and class 9 contains the tallest structures. The structure classes tend to be influenced by higher canopy strata layers as the 95th percentile height increases. Overall canopy cover is generally below 50% in this region, with an exception of polygons in class 3. The canopy cover in class 1 is dominated by the 1-2m, and 4-8m, and 8-

16m strata layers. Classes 2 and 4 have little overall cover. The canopy cover in class 3 is dominated by the 8-16m and 16-32m strata layers. Canopy cover in class 5 is dominated by the 16-32m strata layer. Class 6 is multilayer, with canopy in the 8-16, 16-32, and 32-64m strata layers. Class 7 has low overall cover, but it is canopy is present in cover in the 1-2m to 32-64m strata layers. Class 8 is dominated by canopy in the 8-16, 16-32, and 32-64m strata layers, and class 9 is dominated by canopy in the 32-64m strata layer.

The principal component loadings are shown visually in PC1:PC2 and PC2:PC3 ordination plots. These plots also display the metrics and the structure classes in relation to the loadings (Figures 4 and 5). PC1 is representative of canopy cover in the 32-64 strata layer and the 95th percentile return height, and represents 32% of the variation. PC2 is representative of canopy cover in the 8-16m and 4-8m strata layers, and represents 26% of the variation. PC3 is representative of canopy cover in the 1-2m and 2-4m strata layers, and represents 19% of the variation.

A dendrogram shows the statistical difference among the structural classes. Classes connected by fewer lines and lower connections have less statistical difference. Structure classes 5, 6, 7, 8, and 9 are closely related, and classes 1, 2, 3, and 4 are closely related.

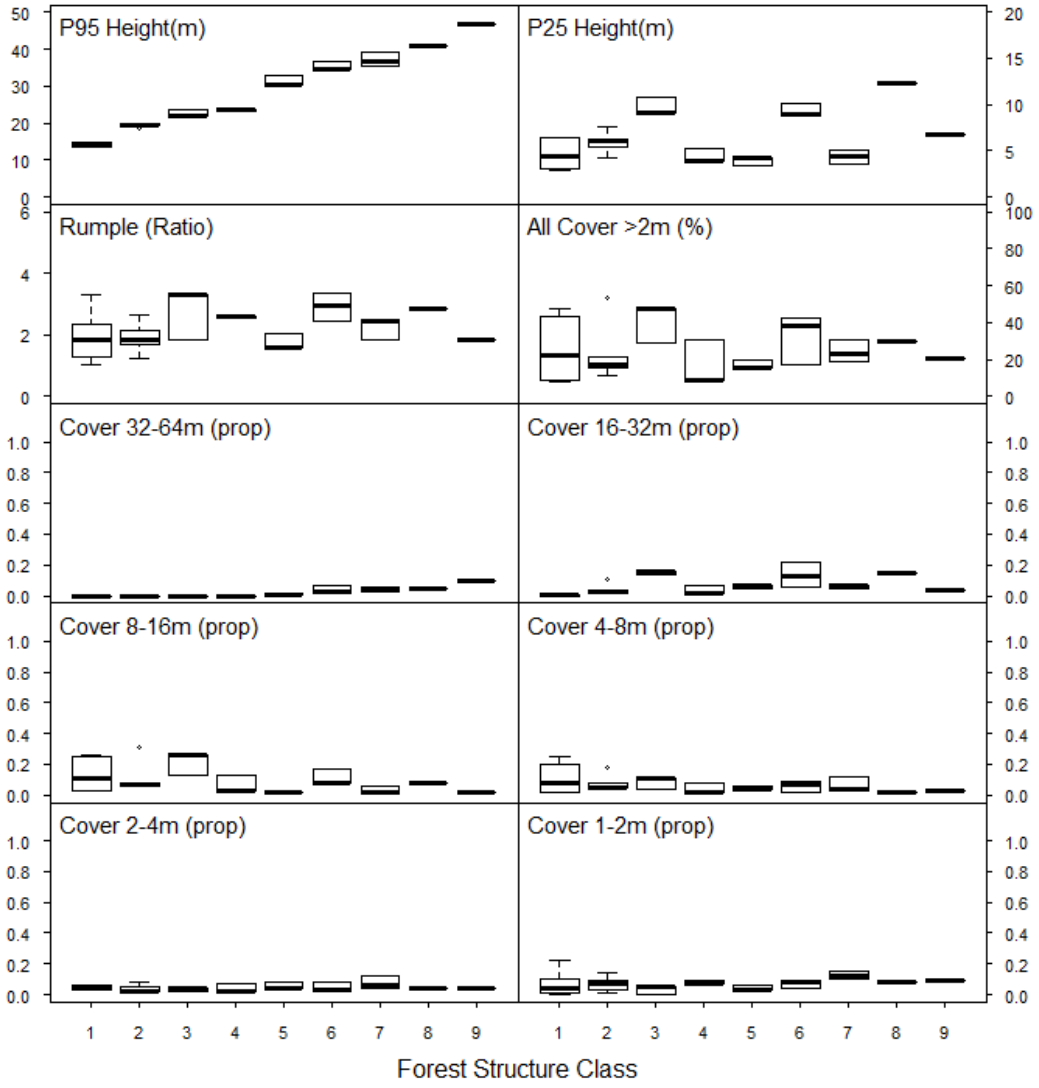

Statistical characteristics of the combined Dinkey2010 and Dinkey 2012 structure class. The classes are ordered by the 95th percentile height, providing a height gradient to compare and contrast the classes.

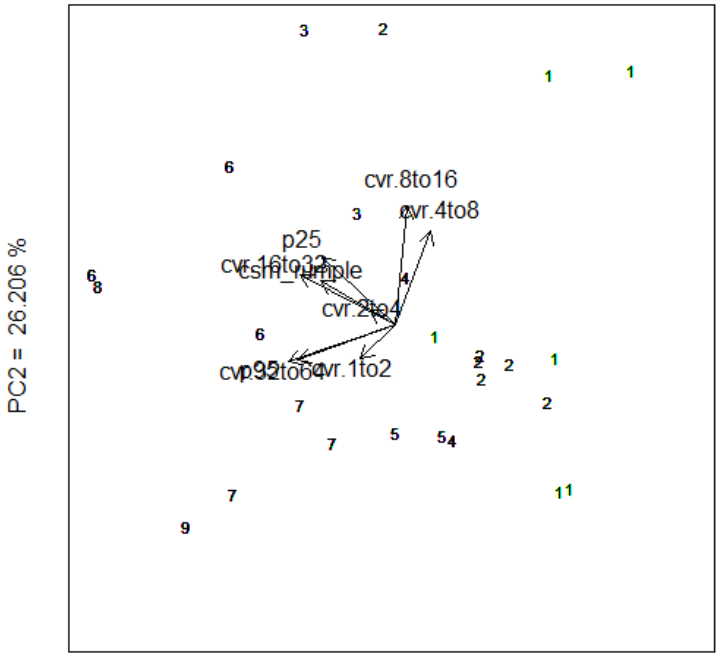

Statistical relationships of the structure classes in relation to PC1 and PC2. Arrow lengths and direction show strength of correlation of a metric with an axis; correlation among metrics is shown by direction of arrows with more closely aligned arrows representing positive correlation, more opposing arrows representing negative correlation, and more perpendicular arrows representing lack of correlation.

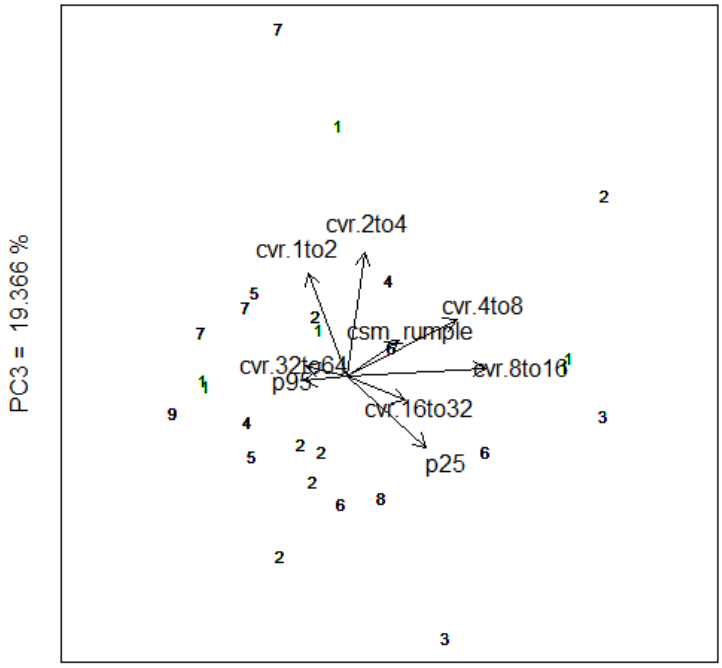

Statistical relationship of the Dinkey Creek classes in relation to PC2 and PC3.

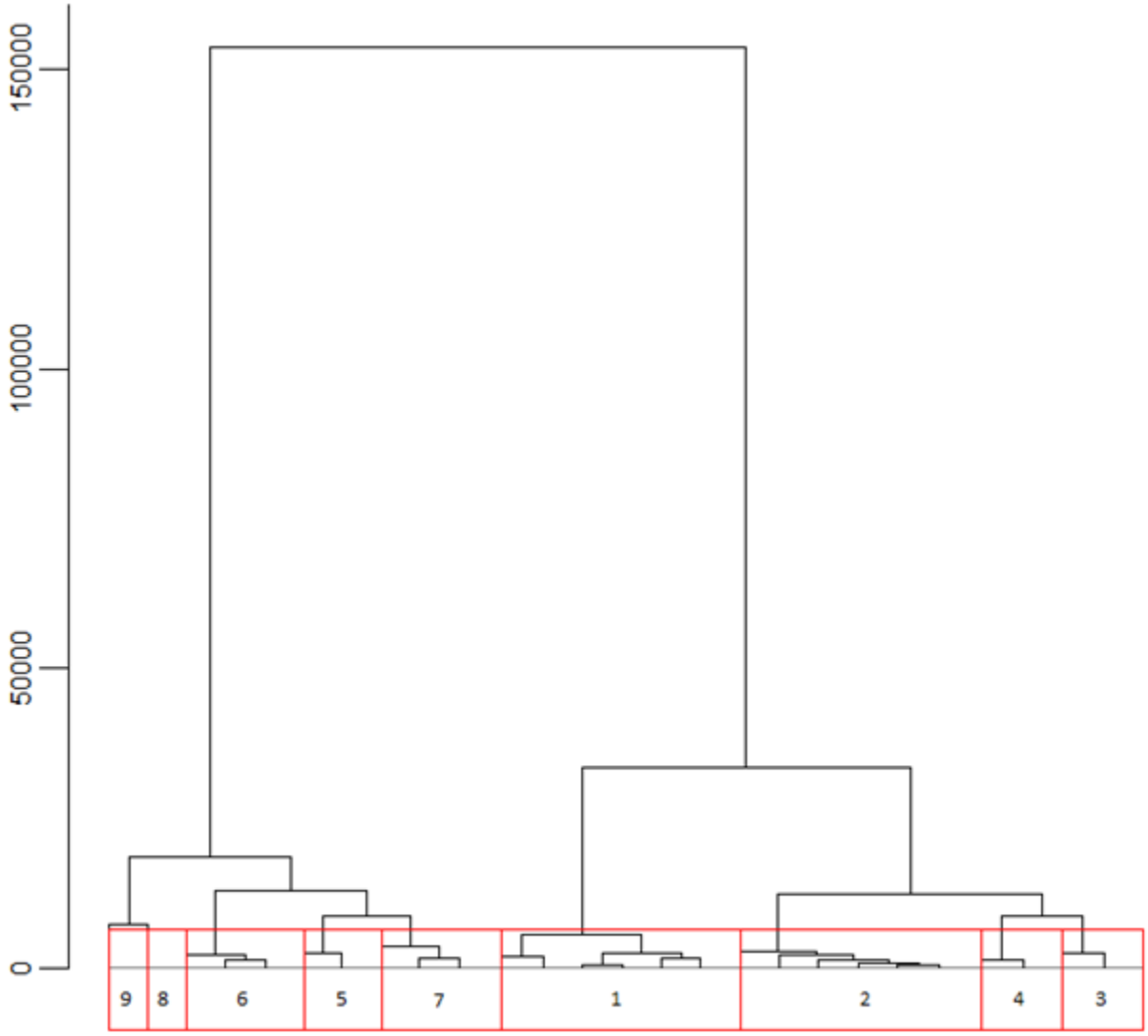

Statistical distance among the combined Dinkey 2010 and 2012 structure classes. Classes connected by fewer lines and lower connections have less statistical difference.

Appendix 3: Comprehensive r^2 lists for the 30-meter resolution flight line comparisons

Data File	Flight Line 106:107	Flight Line 106:1109	Flight Line 39:75
Canopy relief ratio	0.93	0.95	0.96
cover.1.2	0.91	0.95	0.98
cover.16.32	0.99	0.99	1.00
cover.2.4	0.90	0.96	0.83
cover.32.64	0.98	0.99	1.00
cover.4.8	0.93	0.97	0.98
cover.8.16	0.96	0.99	0.99
cover.gt.64	0.22	0.22	0.00
Elev AAD	0.98	0.99	1.00
Elev CURT mean CUBE	0.99	1.00	1.00
Elev CV	0.93	0.97	0.99
Elev IQ	0.95	0.98	0.99
Elev kurtosis	0.89	0.94	0.96
Elev L CV	0.94	0.97	0.99
Elev L kurtosis	0.74	0.93	0.96
Elev L skewness	0.93	0.97	0.96
Elev L1	0.99	0.99	1.00
Elev L2	0.99	0.99	1.00
Elev L3	0.93	0.97	0.98
Elev L4	0.82	0.96	0.97
Elev MAD median	0.95	0.98	0.97
Elev MAD mode	0.75	0.80	0.91
Elev maximum	0.99	0.99	1.00
Elev mean	0.99	0.99	1.00
Elev minimum	0.04	0.14	0.43
Elev mode	0.70	0.68	0.87
Elev P01	0.41	0.49	0.83
Elev P05	0.86	0.91	0.97
Elev P10	0.95	0.97	0.99
Elev P20	0.95	0.96	1.00
Elev P25	0.96	0.98	1.00
Elev P30	0.96	0.99	1.00
Elev P40	0.96	0.99	1.00
Elev P50	0.98	0.99	0.99
Elev P60	0.98	0.99	1.00
Elev P70	0.98	0.99	1.00
Elev P75	0.98	0.99	1.00
Elev P80	0.98	0.99	1.00

Elev P90	0.99	0.99	1.00
Elev P95	0.99	0.99	1.00
Elev P99	1.00	1.00	1.00
Elev skewness	0.94	0.97	0.97
Elev SQRT mean SQ	0.99	1.00	1.00
Elev stddev	0.99	0.99	1.00
Elev strata (1.00 to 2.00) CV	0.34	0.80	0.87
Elev strata (1.00 to 2.00) kurtosis	0.34	0.80	0.87
Elev strata (1.00 to 2.00) max	0.34	0.80	0.87
Elev strata (1.00 to 2.00) mean	0.05	0.38	0.63
Elev strata (1.00 to 2.00) median	0.34	0.80	0.87
Elev strata (1.00 to 2.00) min	0.34	0.80	0.87
Elev strata (1.00 to 2.00) mode	0.34	0.80	0.87
Elev strata (1.00 to 2.00) return proportion	0.93	0.96	0.97
Elev strata (1.00 to 2.00) skewness	0.34	0.80	0.87
Elev strata (1.00 to 2.00) stddev	0.34	0.80	0.87
Elev strata (1.00 to 2.00) total return count	0.86	0.82	0.79
Elev strata (16.00 to 32.00) CV	0.81	0.88	0.97
Elev strata (16.00 to 32.00) kurtosis	0.81	0.88	0.97
Elev strata (16.00 to 32.00) max	0.81	0.88	0.97
Elev strata (16.00 to 32.00) mean	0.99	1.00	0.96
Elev strata (16.00 to 32.00) median	0.81	0.88	0.97
Elev strata (16.00 to 32.00) min	0.81	0.88	0.97
Elev strata (16.00 to 32.00) mode	0.81	0.88	0.97
Elev strata (16.00 to 32.00) return proportion	0.99	0.99	1.00
Elev strata (16.00 to 32.00) skewness	0.81	0.88	0.97
Elev strata (16.00 to 32.00) stddev	0.81	0.88	0.97
Elev strata (16.00 to 32.00) total return count	0.79	0.84	0.65
Elev strata (2.00 to 4.00) CV	1.00	0.33	0.37
Elev strata (2.00 to 4.00) kurtosis	1.00	0.33	0.37
Elev strata (2.00 to 4.00) max	1.00	0.33	0.37
Elev strata (2.00 to 4.00) mean	0.43	0.06	0.01
Elev strata (2.00 to 4.00) median	1.00	0.33	0.37
Elev strata (2.00 to 4.00) min	1.00	0.33	0.37
Elev strata (2.00 to 4.00) mode	1.00	0.33	0.37

Elev strata (2.00 to 4.00) return proportion	0.94	0.96	0.96
Elev strata (2.00 to 4.00) skewness	1.00	0.33	0.37
Elev strata (2.00 to 4.00) stddev	1.00	0.33	0.37
Elev strata (2.00 to 4.00) total return count	0.76	0.81	0.73
Elev strata (32.00 to 64.00) CV	0.91	0.93	0.98
Elev strata (32.00 to 64.00) kurtosis	0.91	0.93	0.98
Elev strata (32.00 to 64.00) max	0.91	0.93	0.98
Elev strata (32.00 to 64.00) mean	1.00	0.96	0.93
Elev strata (32.00 to 64.00) median	0.91	0.93	0.98
Elev strata (32.00 to 64.00) min	0.91	0.93	0.98
Elev strata (32.00 to 64.00) mode	0.91	0.93	0.98
Elev strata (32.00 to 64.00) return proportion	0.98	0.99	1.00
Elev strata (32.00 to 64.00) skewness	0.91	0.93	0.98
Elev strata (32.00 to 64.00) stddev	0.91	0.93	0.98
Elev strata (32.00 to 64.00) total return count	0.84	0.83	0.93
Elev strata (4.00 to 8.00) CV	0.66	0.66	0.44
Elev strata (4.00 to 8.00) kurtosis	0.66	0.66	0.44
Elev strata (4.00 to 8.00) max	0.66	0.66	0.44
Elev strata (4.00 to 8.00) mean	0.30	0.39	0.94
Elev strata (4.00 to 8.00) median	0.66	0.66	0.44
Elev strata (4.00 to 8.00) min	0.66	0.66	0.44
Elev strata (4.00 to 8.00) mode	0.66	0.66	0.44
Elev strata (4.00 to 8.00) return proportion	0.95	0.98	0.98
Elev strata (4.00 to 8.00) skewness	0.66	0.66	0.44
Elev strata (4.00 to 8.00) stddev	0.66	0.66	0.44
Elev strata (4.00 to 8.00) total return count	0.69	0.77	0.68
Elev strata (8.00 to 16.00) CV	0.50	0.50	0.89
Elev strata (8.00 to 16.00) kurtosis	0.50	0.50	0.89
Elev strata (8.00 to 16.00) max	0.50	0.50	0.89
Elev strata (8.00 to 16.00) mean	0.88	0.96	0.94
Elev strata (8.00 to 16.00) median	0.50	0.50	0.89
Elev strata (8.00 to 16.00) min	0.50	0.50	0.89
Elev strata (8.00 to 16.00) mode	0.50	0.50	0.89

Elev strata (8.00 to 16.00) return proportion	0.96	0.98	0.99
Elev strata (8.00 to 16.00) skewness	0.50	0.50	0.89
Elev strata (8.00 to 16.00) stddev	0.50	0.50	0.89
Elev strata (8.00 to 16.00) total return count	0.74	0.75	0.39
Elev strata (above 64.00) CV	0.50	0.50	0.00
Elev strata (above 64.00) kurtosis	0.50	0.50	0.00
Elev strata (above 64.00) max	0.00	0.00	0.00
Elev strata (above 64.00) mean	0.00	0.00	0.00
Elev strata (above 64.00) median	0.00	0.00	0.00
Elev strata (above 64.00) min	0.00	0.00	0.00
Elev strata (above 64.00) mode	0.00	0.00	0.00
Elev strata (above 64.00) return proportion	0.22	0.22	0.00
Elev strata (above 64.00) skewness	0.50	0.50	0.00
Elev strata (above 64.00) stddev	0.00	0.00	0.00
Elev strata (above 64.00) total return count	0.22	0.22	0.00
Elev strata (below 1.00) CV	0.03	0.00	1.00
Elev strata (below 1.00) kurtosis	0.67	0.51	1.00
Elev strata (below 1.00) max	0.27	0.21	1.00
Elev strata (below 1.00) mean	0.96	0.97	0.94
Elev strata (below 1.00) median	0.96	0.97	1.00
Elev strata (below 1.00) min	0.91	0.90	1.00
Elev strata (below 1.00) mode	0.76	0.86	1.00
Elev strata (below 1.00) return proportion	0.99	1.00	0.99
Elev strata (below 1.00) skewness	0.80	0.70	1.00
Elev strata (below 1.00) stddev	0.91	0.94	1.00
Elev strata (below 1.00) total return count	0.50	0.67	0.36
Elev variance	0.99	0.99	1.00
Int AAD	0.78	0.84	0.85
Int CV	0.72	0.62	0.86
Int IQ	0.75	0.78	0.85
Int kurtosis	0.29	0.49	0.75
Int L CV	0.72	0.57	0.87
Int L kurtosis	0.33	0.35	0.81
Int L skewness	0.62	0.72	0.82

Int L1	0.75	0.90	0.83
Int L2	0.76	0.82	0.84
Int L3	0.59	0.71	0.84
Int L4	0.31	0.43	0.79
Int maximum	0.54	0.69	0.45
Int mean	0.75	0.90	0.83
Int mode	0.00	0.00	0.44
Int P01	0.56	0.38	0.23
Int P05	0.63	0.32	0.79
Int P10	0.58	0.29	0.81
Int P20	0.69	0.47	0.90
Int P25	0.70	0.57	0.86
Int P30	0.70	0.69	0.86
Int P40	0.71	0.77	0.85
Int P50	0.70	0.81	0.84
Int P60	0.72	0.87	0.81
Int P70	0.75	0.90	0.79
Int P75	0.74	0.91	0.80
Int P80	0.76	0.91	0.78
Int P90	0.73	0.89	0.78
Int P95	0.70	0.88	0.79
Int P99	0.65	0.77	0.76
Int skewness	0.56	0.69	0.83
Int stddev	0.76	0.82	0.84
Int variance	0.74	0.88	0.82
Return 1 count above 2.00	0.65	0.69	0.21
Return 2 count above 2.00	0.78	0.78	0.43
Return 3 count above 2.00	0.71	0.69	0.58
Return 4 count above 2.00	0.35	0.16	0.15
Total return count	0.06	0.19	0.09
Total return count above 2.00	0.68	0.71	0.21

Appendix 4: Comprehensive R^2 list for the 30-meter resolution Dinkey 2010:Dinkey 2012 comparisons

Metric	Overall Area	Unharvested Area	Harvested Area
1st_cnt_above_mean_30METERS.asc	0.36	0.35	0.46
1st_cnt_above_mode_30METERS.asc	0.32	0.33	0.31
1st_cnt_above2_30METERS.asc	0.32	0.31	0.40
1st_cover_above_mean_30METERS.asc	0.96	0.97	0.87
1st_cover_above_mode_30METERS.asc	0.77	0.82	0.56
1st_cover_above2_30METERS.asc	0.96	0.97	0.85
all_1st_cover_above_mean_30METERS.asc	0.95	0.97	0.87
all_1st_cover_above_mode_30METERS.asc	0.75	0.81	0.55
all_1st_cover_above2_30METERS.asc	0.95	0.97	0.84
all_cnt_2plus_30METERS.asc	0.34	0.33	0.42
all_cnt_30METERS.asc	0.02	0.02	0.02
all_cnt_above_mean_30METERS.asc	0.37	0.35	0.46
all_cnt_above_mode_30METERS.asc	0.33	0.34	0.32
all_cnt_above2_30METERS.asc	0.34	0.33	0.42
all_cover_above_mean_30METERS.asc	0.96	0.97	0.87
all_cover_above_mode_30METERS.asc	0.74	0.79	0.52
all_cover_above2_30METERS.asc	0.95	0.97	0.84
canopy_30METERS_average_height.asc	0.90	0.92	0.82
canopy_30METERS_FPV.asc	0.83	0.86	0.76
canopy_30METERS_maximum_height.asc	0.88	0.91	0.79
canopy_30METERS_rumple.asc	0.89	0.92	0.81
canopy_30METERS_stddev_height.asc	0.87	0.90	0.79
Cover_1-2m.asc	0.79	0.82	0.53
Cover_16-32m.asc	0.97	0.98	0.90
Cover_2-4m.asc	0.87	0.91	0.47
Cover_32-64m.asc	0.98	0.98	0.97
Cover_4-8m.asc	0.88	0.92	0.59
Cover_8-16m.asc	0.92	0.95	0.72
Cover_gt64m.asc	0.91	0.86	0.97
Dinkey2010_classification_9_classes_2014-12-02.asc	0.54	0.61	0.39
elev_AAD_2plus_30METERS.asc	0.98	0.99	0.94
elev_ave_2plus_30METERS.asc	0.98	0.98	0.96
elev_canopy_relief_ratio_30METERS.asc	0.90	0.91	0.85
elev_cubic_mean_30METERS.asc	0.99	0.99	0.97
elev_CV_2plus_30METERS.asc	0.90	0.92	0.82
elev_IQ_2plus_30METERS.asc	0.96	0.97	0.90
elev_kurtosis_2plus_30METERS.asc	0.11	0.41	0.19
elev_L1_2plus_30METERS.asc	0.98	0.98	0.96

elev_L2_2plus_30METERS.asc	0.98	0.99	0.95
elev_L3_plus_30METERS.asc	0.91	0.91	0.87
elev_L4_2plus_30METERS.asc	0.85	0.87	0.77
elev_LCV_2plus_30METERS.asc	0.90	0.93	0.81
elev_Lkurtosis_2plus_30METERS.asc	0.72	0.77	0.67
elev_Lskewness_2plus_30METERS.asc	0.89	0.91	0.87
elev_MAD_median_30METERS.asc	0.95	0.96	0.89
elev_MAD_mode_30METERS.asc	0.73	0.79	0.60
elev_max_2plus_30METERS.asc	0.97	0.98	0.95
elev_min_2plus_30METERS.asc	0.72	0.94	0.08
elev_mode_2plus_30METERS.asc	0.74	0.78	0.66
elev_P01_2plus_30METERS.asc	0.71	0.84	0.52
elev_P05_2plus_30METERS.asc	0.86	0.91	0.75
elev_P10_2plus_30METERS.asc	0.90	0.94	0.82
elev_P20_2plus_30METERS.asc	0.94	0.96	0.88
elev_P25_2plus_30METERS.asc	0.95	0.96	0.90
elev_P30_2plus_30METERS.asc	0.95	0.96	0.91
elev_P40_2plus_30METERS.asc	0.96	0.97	0.93
elev_P50_2plus_30METERS.asc	0.97	0.98	0.95
elev_P60_2plus_30METERS.asc	0.97	0.98	0.96
elev_P70_2plus_30METERS.asc	0.98	0.98	0.96
elev_P75_2plus_30METERS.asc	0.98	0.99	0.97
elev_P80_2plus_30METERS.asc	0.98	0.99	0.97
elev_P90_2plus_30METERS.asc	0.99	0.99	0.97
elev_P95_2plus_30METERS.asc	0.99	0.99	0.98
elev_P99_2plus_30METERS.asc	0.99	0.99	0.98
elev_quadratic_mean_30METERS.asc	0.98	0.99	0.97
elev_skewness_2plus_30METERS.asc	0.86	0.89	0.88
elev_stddev_2plus_30METERS.asc	0.98	0.99	0.96
elev_variance_2plus_30METERS.asc	0.98	0.98	0.95
int_AAD_2plus_30METERS.asc	0.45	0.48	0.44
int_ave_2plus_30METERS.asc	0.41	0.42	0.54
int_CV_2plus_30METERS.asc	0.37	0.38	0.28
int_IQ_2plus_30METERS.asc	0.01	0.01	0.01
int_kurtosis_2plus_30METERS.asc	0.17	0.30	0.19
int_L1_2plus_30METERS.asc	0.41	0.42	0.54
int_L2_2plus_30METERS.asc	0.01	0.02	0.00
int_L3_2plus_30METERS.asc	0.06	0.08	0.06
int_L4_2plus_30METERS.asc	0.00	0.00	0.00
int_LCV_2plus_30METERS.asc	0.01	0.01	0.02
int_Lkurtosis_2plus_30METERS.asc	0.00	0.00	0.00

int_Lskewness_2plus_30METERS.asc	0.00	0.00	0.00
int_max_2plus_30METERS.asc	0.14	0.15	0.09
int_min_2plus_30METERS.asc	0.17	0.19	0.01
int_mode_2plus_30METERS.asc	0.22	0.24	0.25
int_P01_2plus_30METERS.asc	0.00	0.00	0.00
int_P05_2plus_30METERS.asc	0.00	0.00	0.00
int_P10_2plus_30METERS.asc	0.00	0.00	0.00
int_P20_2plus_30METERS.asc	0.00	0.00	0.00
int_P25_2plus_30METERS.asc	0.00	0.00	0.00
int_P30_2plus_30METERS.asc	0.00	0.00	0.00
int_P40_2plus_30METERS.asc	0.00	0.00	0.00
int_P50_2plus_30METERS.asc	0.00	0.00	0.00
int_P60_2plus_30METERS.asc	0.00	0.00	0.00
int_P70_2plus_30METERS.asc	0.00	0.00	0.00
int_P75_2plus_30METERS.asc	0.00	0.00	0.00
int_P80_2plus_30METERS.asc	0.00	0.00	0.00
int_P90_2plus_30METERS.asc	0.00	0.00	0.00
int_P95_2plus_30METERS.asc	0.01	0.01	0.00
int_P99_2plus_30METERS.asc	0.02	0.02	0.01
int_skewness_2plus_30METERS.asc	0.42	0.44	0.44
int_stddev_2plus_30METERS.asc	0.40	0.43	0.40
int_variance_2plus_30METERS.asc	0.37	0.39	0.36
pulsecnt_30METERS.asc	0.01	0.00	0.00
r1_cnt_2plus_30METERS.asc	0.32	0.31	0.40
r2_cnt_2plus_30METERS.asc	0.46	0.44	0.53
r3_cnt_2plus_30METERS.asc	0.50	0.47	0.56
r4_cnt_2plus_30METERS.asc	0.38	0.37	0.40
r5_cnt_2plus_30METERS.asc	0.00	0.00	0.00
strata1_CV_30METERS.asc	0.00	0.00	0.00
strata1_kurtosis_30METERS.asc	0.21	0.44	0.06
strata1_max_30METERS.asc	0.45	0.52	0.38
strata1_mean_30METERS.asc	0.26	0.28	0.25
strata1_median_30METERS.asc	0.20	0.22	0.19
strata1_min_30METERS.asc	0.20	0.14	0.05
strata1_mode_30METERS.asc	0.06	0.07	0.02
strata1_return_proportion_30METERS.asc	0.94	0.96	0.82
strata1_skewness_30METERS.asc	0.56	0.61	0.34
strata1_stddev_30METERS.asc	0.66	0.67	0.58
strata1_total_return_cnt_30METERS.asc	0.21	0.19	0.28
strata2_CV_30METERS.asc	0.18	0.22	0.08
strata2_kurtosis_30METERS.asc	0.24	0.30	0.04

strata2_max_30METERS.asc	0.27	0.35	0.10
strata2_mean_30METERS.asc	0.52	0.59	0.26
strata2_median_30METERS.asc	0.48	0.56	0.24
strata2_min_30METERS.asc	0.17	0.19	0.14
strata2_mode_30METERS.asc	0.25	0.30	0.10
strata2_return_proportion_30METERS.asc	0.77	0.79	0.67
strata2_skewness_30METERS.asc	0.46	0.53	0.23
strata2_stddev_30METERS.asc	0.15	0.18	0.03
strata2_total_return_cnt_30METERS.asc	0.49	0.50	0.52
strata3_CV_30METERS.asc	0.29	0.31	0.18
strata3_kurtosis_30METERS.asc	0.22	0.24	0.16
strata3_max_30METERS.asc	0.46	0.55	0.18
strata3_mean_30METERS.asc	0.58	0.64	0.34
strata3_median_30METERS.asc	0.53	0.58	0.32
strata3_min_30METERS.asc	0.24	0.30	0.16
strata3_mode_30METERS.asc	0.17	0.20	0.08
strata3_return_proportion_30METERS.asc	0.91	0.92	0.57
strata3_skewness_30METERS.asc	0.49	0.52	0.30
strata3_stddev_30METERS.asc	0.29	0.32	0.16
strata3_total_return_cnt_30METERS.asc	0.53	0.55	0.39
strata4_CV_30METERS.asc	0.55	0.57	0.35
strata4_kurtosis_30METERS.asc	0.40	0.50	0.24
strata4_max_30METERS.asc	0.72	0.67	0.69
strata4_mean_30METERS.asc	0.76	0.77	0.54
strata4_median_30METERS.asc	0.70	0.74	0.48
strata4_min_30METERS.asc	0.31	0.25	0.15
strata4_mode_30METERS.asc	0.25	0.31	0.14
strata4_return_proportion_30METERS.asc	0.92	0.94	0.72
strata4_skewness_30METERS.asc	0.65	0.68	0.46
strata4_stddev_30METERS.asc	0.62	0.63	0.37
strata4_total_return_cnt_30METERS.asc	0.46	0.45	0.44
strata5_CV_30METERS.asc	0.84	0.85	0.61
strata5_kurtosis_30METERS.asc	0.59	0.55	0.52
strata5_max_30METERS.asc	0.90	0.90	0.76
strata5_mean_30METERS.asc	0.92	0.93	0.81
strata5_median_30METERS.asc	0.90	0.92	0.79
strata5_min_30METERS.asc	0.45	0.43	0.53
strata5_mode_30METERS.asc	0.48	0.54	0.38
strata5_return_proportion_30METERS.asc	0.94	0.95	0.83
strata5_skewness_30METERS.asc	0.81	0.80	0.74
strata5_stddev_30METERS.asc	0.89	0.89	0.71

strata5_total_return_cnt_30METERS.asc	0.42	0.40	0.48
strata6_CV_30METERS.asc	0.94	0.94	0.91
strata6_kurtosis_30METERS.asc	0.64	0.60	0.71
strata6_max_30METERS.asc	0.96	0.96	0.94
strata6_mean_30METERS.asc	0.97	0.97	0.95
strata6_median_30METERS.asc	0.95	0.96	0.94
strata6_min_30METERS.asc	0.57	0.69	0.26
strata6_mode_30METERS.asc	0.64	0.67	0.59
strata6_return_proportion_30METERS.asc	0.97	0.98	0.90
strata6_skewness_30METERS.asc	0.83	0.84	0.87
strata6_stddev_30METERS.asc	0.96	0.96	0.94
strata6_total_return_cnt_30METERS.asc	0.51	0.50	0.59
strata7_CV_30METERS.asc	0.95	0.96	0.93
strata7_kurtosis_30METERS.asc	0.28	0.46	0.13
strata7_max_30METERS.asc	0.96	0.97	0.94
strata7_mean_30METERS.asc	0.95	0.96	0.94
strata7_median_30METERS.asc	0.95	0.95	0.93
strata7_min_30METERS.asc	0.50	0.56	0.70
strata7_mode_30METERS.asc	0.57	0.62	0.57
strata7_return_proportion_30METERS.asc	0.98	0.98	0.97
strata7_skewness_30METERS.asc	0.58	0.61	0.55
strata7_stddev_30METERS.asc	0.96	0.97	0.94
strata7_total_return_cnt_30METERS.asc	0.69	0.65	0.83
strata8_CV_30METERS.asc	0.92	0.95	0.73
strata8_kurtosis_30METERS.asc	0.24	0.34	0.10
strata8_max_30METERS.asc	0.94	0.94	0.91
strata8_mean_30METERS.asc	0.45	0.11	0.92
strata8_median_30METERS.asc	0.88	0.79	0.88
strata8_min_30METERS.asc	0.55	0.94	0.54
strata8_mode_30METERS.asc	0.49	0.28	0.76
strata8_return_proportion_30METERS.asc	0.91	0.86	0.97
strata8_skewness_30METERS.asc	0.31	0.31	0.09
strata8_stddev_30METERS.asc	0.92	0.95	0.74
strata8_total_return_cnt_30METERS.asc	0.76	0.80	0.95
topo_aspect_30METERS.asc	0.96	0.95	0.94
topo_curvature_30METERS.asc	0.88	0.83	0.89
topo_elevation_30METERS.asc	1.00	1.00	1.00
topo_plancurv_30METERS.asc	0.88	0.84	0.88
topo_profilecurv_30METERS.asc	0.88	0.84	0.90
topo_slope_30METERS.asc	1.00	0.99	1.00
topo_sri_30METERS.asc	1.00	1.00	1.00